ISSN 2095-9273
CN 10-1298/N

Science Bulletin

Volume 62 · Number 12 · June 2017

ELSEVIER
SCIENCE CHINA PRESS
Chinese Academy of Sciences
National Natural Science Foundation of China

Science Bulletin 62 (2017) 820–830

Contents lists available at ScienceDirect

Science Bulletin

journal homepage: www.elsevier.com/locate/scib

Article

The RNA editome of *Macaca mulatta* and functional characterization of RNA editing in mitochondria

Ling-Qun Ye [a,d,1], Hui Zhao [b,1], He-Jiang Zhou [c,f,1], Xiao-Die Ren [a,d,1], Lin-Lin Liu [b,1], Newton O. Otecko [a,d], Zheng-bo Wang [c], Min-Min Yang [a], Lin Zeng [a,d], Xin-Tian Hu [c,e], Yong-Gang Yao [c,d,e,f], Ya-Ping Zhang [a,d,*], Dong-Dong Wu [a,d,e,*]

[a] State Key Laboratory of Genetic Resources and Evolution, Kunming Institute of Zoology, Chinese Academy of Sciences, Kunming 650223, China
[b] State Key Laboratory for Conservation and Utilization of Bio-Resources in Yunnan, Yunnan University, Kunming 650091, China
[c] Key Laboratory of Animal Models and Human Disease Mechanisms of Chinese Academy of Sciences & Yunnan Province, Kunming Institute of Zoology, Chinese Academy of Sciences, Kunming 650223, China
[d] Kunming College of Life Science, University of Chinese Academy of Sciences, Kunming 650204, China
[e] Kunming Primate Research Center of the Chinese Academy of Sciences, Kunming Institute of Zoology, Chinese Academy of Sciences, Kunming 650223, China
[f] CAS Center for Excellence in Brain Science and Intelligence Technology, Chinese Academy of Sciences, Shanghai 200031, China

ARTICLE INFO

Article history:
Received 28 April 2017
Received in revised form 9 May 2017
Accepted 16 May 2017
Available online 19 May 2017

ABSTRACT

RNA editing was first discovered in mitochondrial RNA molecular. However, whether adenosine-to-inosine (A-to-I) RNA editing has functions in nuclear genes involved in mitochondria remains elusive. Here, we retrieved 707,246 A-to-I RNA editing sites in *Macaca mulatta* leveraging massive transcriptomes of 30 different tissues and genomes of nine tissues, together with the reported data, and found that A-to-I RNA editing occurred frequently in nuclear genes that have functions in mitochondria. The mitochondrial structure, the level of ATP production, and the expression of some key genes involved in mitochondrial function were dysregulated after knocking down the expression of *ADAR1* and *ADAR2*, the key genes encoding the enzyme responsible for RNA editing. When investigating dynamic changes of RNA editing during brain development, an amino-acid-changing RNA editing site (I234/V) in *MFN1*, a mediator of mitochondrial fusion, was identified to be significantly correlated with age, and could influence the function of MFN1. When studying transcriptomes of brain disorder, we found that dysregulated RNA editing sites in autism were also enriched within genes having mitochondrial functions. These data indicated that RNA editing had a significant function in mitochondria via their influence on nuclear genes.

1. Introduction

Adenosine-to-inosine (A-to-I) RNA editing is a widespread phenomenon in animals whose consequences include an increased level of transcriptome diversity [1–3]. It is a catalytic post- or co-transcriptional modification of nucleotide from adenosine to inosine in RNA carried out by the adenosine deaminase acting on the RNA (ADAR) family of enzymes [1–3]. Studies of the ADAR family indicate that adenosine-to-inosine (A-to-I) RNA editing has crucial and broad functions. For example, mammals carry three members of the ADAR family: ADAR1 and ADAR2, and ADAR3 (also known as ADAR, ADARB1, and ADARB2, respectively) [2]. In mouse, *Adar1*$^{-/-}$ embryos die between E11.5 and E12.5 as a result of failure to maintain hematopoiesis [4]. *Adar2*$^{-/-}$ mice develop epileptic seizures and die a few weeks after birth [5]. In *Drosophila melanogaster*, *ADAR* knock out leads to uncoordinated locomotion, temperature-sensitive paralysis, and age-dependent neurodegeneration [6]. In *Caenorhabditis elegans*, ADARs including ADR1 and ADR2 are essential for normal behavior, and deletion of the genes induces defective chemotaxis [7].

The most important impact of A-to-I RNA editing pertains to the nervous system [3,8–10]. Dysregulation of RNA editing can induce a variety of diseases of the nervous system [11–14]. For example, the editing level of the glutamate receptor GluA2 Q/R site might be altered in epilepsy, amyotrophic lateral sclerosis, malignant glioma, schizophrenia, and ischemia [3,11]. Dysregulated 5-HT2CR mRNA editing might be involved in depression and suicide, schizophrenia, Prader–Willi syndrome, and metabolic diseases such as obesity and diabetes [3,15]. Additionally, several recent studies have revealed dysregulation of A-to-I RNA editing in many tumors, and some editing sites play a role in tumorigenesis [16–

* Corresponding authors.
E-mail addresses: zhangyp@mail.kiz.ac.cn (Y.-P. Zhang), wudongdong@mail.kiz.ac.cn (D.-D. Wu).
[1] These authors contributed equally to this work.

http://dx.doi.org/10.1016/j.scib.2017.05.021
2095-9273/

20]. Furthermore, A-to-I RNA editing has also been reported to have important effects on the innate immunity [21–23].

Accumulating experiments support broad and important functions of RNA editing. It is acknowledged that RNA editing was first discovered in mitochondrial RNA molecules [24], and mitochondrial C-to-U RNA editing has been observed in plants [25], heteroloboseans [26,27] and metazoans [28,29]. We hypothesized that A-to-I RNA editing might also have a function in mitochondria. In the present study, we constructed the primate editome of *Macaca mulatta*. We focused on nuclear genes involved in mitochondrial functions that are subject to A-to-I editing, and characterized the functions of RNA editing in mitochondria by influencing nuclear genes involved in mitochondrial function.

2. Materials and methods

2.1. Ethics statement

The handling the rhesus macaque used in this study followed the guidelines and regulations of Kunming Institute of Zoology (KIZ) on animal experimentation and was approved by the Institutional Animal Care and Use Committee of the KIZ.

2.2. Genome and transcriptome generated in this study

The genomes from nine different tissues, and unstranded transcriptomes of 30 different tissues from a 25 years old rhesus macaque were sequenced by Illumina Hiseq platform. In total, 2.76 billion DNA reads and 2.20 billion RNA reads were generated, which were used to call RNA editing sites in rhesus macaque.

2.3. RNA editome in the rhesus macaque

RNA reads from different tissues were pooled together to call RNA variants based on our previously published pipeline (Fig. S1) [30]. Many quality control steps were performed to filter potential false-positive sites (Fig. S1), modified from previous pipelines [30–32]. Human editing sites were downloaded from the RADAR database (http://rnaedit.com/) [33], and our previous study [30]. We used the LiftOver program from UCSC Genome Browser (https://genome.ucsc.edu/) to convert genomic positions between human and rhesus macaque. The editing sites shared between human and rhesus macaque were deemed as conserved editing sites. RNA editing level was calculated as the proportion of edited reads out of all mapped reads at a given site.

2.4. Transcriptomic data of rhesus macaque from other studies

In order to study the dynamic pattern of editing level in different biological processes, many transcriptomes from different projects were downloaded from previous studies [34–36]. Detailed information about generation of the transcriptome data can be found in the original publications. In brief, transcriptomic data of prefrontal cortex from 39 male macaques, with age range from −56 day to 21 years 8 days (minus indicate days before birth) were retrieved from a previous study by He et al. [34]. Transcriptome data from different tissues including brain, colon, heart, kidney, liver, lung, skeletal muscle, spleen, and testes were taken from a previous study by Merkin et al. [35]. Transcriptomic data during differentiation of embryonic stem cells into neural stem cells were taken from a previous study by Zhao and coworkers [36].

2.5. RNA editing in brain disorder

The prefrontal cortex transcriptomes of 34 autism cases (2–60 years old) and 40 controls (0–62 years old), sequenced by RNA-sequencing were taken from a previous study by Liu and coworkers [37]. Detailed information about sampling and sequencing can be found in the original publication. Human editing sites were downloaded from the RADAR database (http://rnaedit.com/) [33] and our previous study [30]. Editing level of each site within each tissue was calculated, and tissues containing reads covering the sites lower than 5 were discarded. Significance of differential RNA level between case and control was calculated by the generalized linear models function in R, adjusted for age, sex and gene expression value.

2.6. ADAR gene knock-down experiments

U251 glioma cells were introduced from the Kunming Cell Bank, KIZ, and were cultured in Roswell RPMI-1640 medium (HyClone, Logan, UT) supplemented with 10% fetal bovine serum, 100 U/mL penicillin and 100 g/mL streptomycin in 5% CO_2 at 37 °C. Transfection with siRNA was performed using an electroporator (CUY21EDIT, Nepa gene, Japan). After electroporation, cells were seeded in normal growth medium for 48 h and then used in experiments. Appropriately same amount of treated cells were washed once with 1X PBS followed by addition of lysis buffer (Beyotime, China) at 4 °C for 30 min. After centrifugation at 12,000 *g* for 15 min, the supernatant was collected. Proteins (25 μg) were separated on 12% (w/v) SDS-polyacrylamide gels and transferred to a polyvinylidene difluoride membrane (Roche, USA) using a BioRad semi-dry transfer apparatus. The membrane was soaked with 5% (w/v) skim milk for 2 h at room temperature and then incubated with primary antibodies against ADAR1 (Merck Millipore, MABE888; 1:1000), ADAR2 (Merck Millipore, MABE889; 1:1000), Mfn1 (Abcam Inc., ab57602, 1:1000), TIM23 (Proteintech, 11123-1-AP; 1:2000), Tom20 (Cell Signaling Technology, #42406 s; 1:2000), CoxIV (Cell Signaling Technology, #4850p, 1:2000), VDAC1 (Merck Millipore, MABN504; 1:2000), and GAPDH (Proteintech, 60004-I-IG; 1:20,000) overnight at 4 °C. After three washes with TBST (each wash 5 min), the membrane was incubated with anti-mouse or anti-rabbit IgG peroxidase-conjugated secondary antibody (KPL, Gaithersburg, MD, USA) (1:10,000) for 1 h at room temperature. Immobilon Western Chemiluminescent HRP Substrate (Millipore, USA) was used to visualize the epitope.

2.7. Confocal fluorescence microscopy

Confocal fluorescence microscopy was used to investigate the expression levels of ADAR1 or ADAR2 and mitochondrial morphology. After electroporation with siRNA 48 h, U251 cells were incubated with 50 nmol/L MitoTracker (Life Technologies; M7512; USA) washed thrice with 1X PBS and then fixed with paraformaldehyde (PFA; 4% (w/v)) in phosphate-buffered saline (PBS) for 10 min. The cells were then permeabilized using 0.2% (v/v) Triton X-100, followed by a block in 5% (w/v) bovine serum albumin 1 h at room temperature. Cells were incubated with primary antibody (anti-ADAR1 or anti-ADAR2) overnight at 4 °C, then with a FITC-conjugated secondary antibody (KPL, 1:50) for 1 h at room temperature after three washes with PBS. 4′,6-Diamidino-2-phenylindole (DAPI) (Roche, USA) was used to color the nucleus. Cells imaging was done using the Olympus FluoView™ 1000 confocal microscope (Olympus, Melville, NY, USA) at 488 and 563 nm, respectively.

2.8. Measurement of mitochondrial mass level

For mitochondrial mass measurement, U251 cells were harvested 72 h after transfection with the indicated siRNA, and then incubated in prewarm medium with 100 nmol/L MitoTracker Red FM (Molecular Probe, USA, M22425) at 37 °C for 30 min, then washed with prewarmed PBS and analyzed by using flow cytometry (BD) at 644 nm.

2.9. Determination of cellular ATP level

U251 cells were seeded in 12-well plates after transfection with the indicated siRNA. Forty-eight hours later, cells were lysed in 100 μL lysis buffer (GENMED, China, GMS10050). 10 μL of cell lysate was used to measure cellular ATP level per the manufacture's manual for ATP Determination Kit (Invitrogen) on a GloMax 96 Luminometer (Promega). The final ATP value was normalized to the protein concentration of each sample.

2.10. Functional characterization of MFN1 I234/V

The pcDNA3.1/myc-His(−) A plasmid (Invitrogen, CA, USA) was used to construct the expression plasmid. This plasmid was digested with *Xho*I and *Kpn*I to prepare the cloning vector. For insert preparation, PCR was performed to obtain the full-length MFN1 cDNA using the forward primer 5′-ATGCTGTGGGA TAAAGTTCTCCCTA-3′ and reverse primer 5′-GGATTCTTCATTGCTT GAAGGTAGAA-3′. Subsequently, PCR was performed to attach the tag using forward primer 5′-CTCGAGGAGCAGAAACTCATCTCTGAA GAGGATCTGGAGCAGAAACTCATCTCTGAAGAGGATCTGGAGCAGAA ACTCATCTCTGAAGAGGATCTGGAGCAGAAACTCATCTCTGAAGAGGA TCTGGAGCAGAAACTCATCTCTGAAGAGGATCTGGAGCAGAAACTCAT CTCTGAAGAGGATCTGATGCTGTGGGATAAAGTTCTC-3′ (*Xho*I and 6×myc tag attached) and reverse primer 5′-GGTACCCTTATCGTCGT CATCCTTGTAATCCTTATCGTCGTCATCCTTGTAATCCTTATCGTCGTCA TCCTTGTAATCCTTATCGTCGTCATCCTTGTAATCCTTATCGTCGTCATC CTTGTAATCCTTATCGTCGTCATCCTTGTAATCGGATTCTTCATTGCTTG AAGG (*Kpn*I site and 6×FLAG tag attached). The products were then digested with *Xho*I and *Kpn*I and cloned into the prepared vector to generate the pcDNA3-MFN1 plasmid. The MFN1 RNA editing fragment was produced by PCR using the pcDNA3-MFN1 plasmid as a template by a PCR-based approach, and similar steps as stated above were used to generate the pcDNA3-MFN1(I234/V) plasmid.

The human glioblastoma T98G cell line was provided by the American Type Culture Collection (ATCC; Rockville, MD, USA) and maintained in Modified Eagle's Medium (MEM, Thermo, Beijing, China) supplemented with 10% fetal bovine serum (FBS), 1% penicillin, and streptomycin (Invitrogen, Beijing, China). The constructed plasmids were transfected into T98G cells using X-tremeGENE HP DNA transfection reagent following the manufacturer's manual (Roche, Mannheim, Germany). The T98G cells transfected with pcDNA3-MFN1 or pcDNA3-MFN1 (I234/V) plasmids were dissolved in radioimmunoprecipitation assay (RIPA) buffer (Pierce, IL, USA) with the addition of EDTA-free protease inhibitor Cocktail Tablets (Roche, Mannheim, Germany). Protein concentration in the supernatant was determined by the bicinchoninic acid (BCA) protein assay kit (Thermo, IL, USA). The cell lysate was subjected to SDS-PAGE and transferred onto polyvinylidene fluoride (PVDF) membranes (Millipore, MA, USA). The membranes were incubated with anti-myc antibody (1:1000, Clontech, Mountain Valley, CA), anti-FLAG monoclonal antibody (1:1000, Sigma, MO, USA), or anti-actin monoclonal antibody (1:1000, Cell Signaling Technology, MA, USA) and subsequently incubated with horseradish peroxidase-conjugated secondary antibody (1:5000, Santa Cruz Biotechnology Inc. California, USA). Immunoreactive bands were visualized by SuperSignalWest Pico Chemiluminescent Substrate (Thermo, IL, USA) using an Amersham Imager 600 (GE, Tokyo, Japan).

2.11. Cell viability and apoptosis assays

Cell viability was measured by the Sulforhodamine B (SRB, Sigma, St. Louis, MO) assay per a previous report [38]. In brief, T98G cells were seeded into 12-well plates and then transfected after 24 h. After transfection for 0, 24, 48, and 72 h, the cells were fixed and washed. Finally, Tris-base buffer was added to each well, and optical densities at 530 nm were measured by a spectrophotometric plate reader. Cell apoptosis was analyzed using Caspase-3 Colorimetric Assay (RD Pharmingen, San Diego, CA) per the company's protocol. Briefly, T98G cells were transfected with pcDNA3-MFN1or pcDNA3-MFN1(I234/V). After transfection for 48 h, the control and experimental cells were harvested, mixed with 50 μL of cell lysis buffer and kept on ice for 10 min. Subsequently, 50 μL of 2x Reaction Buffer 3, containing 10 mmol/L DTT and 5 μL of caspase-3 colorimetric substrate (DEVD-pNA), were added to each of the supernatant cytosolic extracts. After a 1.5 h incubation at 37 °C, the absorbance of samples was measured at 405 nm.

3. Results

3.1. Evaluating the influence of sequence coverage on RNA editing calling

In the study by Chen et al. [39], only 31,250 A-to-I RNA-editing sites were identified in rhesus macaque [39], much fewer compared to human containing millions of editing sites [3,30]. In the present study, we firstly constructed an exhaustive editome of primate to facilitate the investigation of function of A-to-I RNA editing.

As A-to-I RNA editing is prominent in nervous system, we reason that more data from more different brain structures will undoubtedly facilitate the detection of RNA editing in the primate. In addition, many somatic mutations identified in different tissues (Table S1) could cause false positive, which has not been considered in the previous studies. Accordingly, to build a comprehensive editome of the rhesus macaque, more than 1.96 billion reads from 30 tissue samples (including 21 tissues from different brain structures) from a 25 years old rhesus macaque were generated by deep RNA sequencing (Table S2), and another nine genomes from nine different tissues of the same donor were sequenced with more than 80X depth (Table S1). We leveraged a pipeline modified from previous studies [30,31], to separately call RNA editing sites at Alu and non-Alu regions in the genome of the rhesus macaque based on transcriptomic and genomic data (Fig. S1). Mapped RNA reads from all tissues were pooled to increase the sequence coverage for calling RNA-DNA difference sites (RDDs) (Fig. S1), whereas DNA mapped reads from the same individual were used to filter out sites of DNA mutations.

We firstly evaluated the influence of sequence coverage of the transcriptome on the number of identified editing sites [31,40] based on randomly selected reads. More A-to-G/T-to-C RDDs were called in both Alu and non-Alu regions when more reads were used, as previously reported in humans [41], whereas other types of RDDs were negligible (Fig. 1a, b). The proportion of A-to-G/T-to-C RDDs was very high in the Alu region and increased rapidly in the non-Alu region when more reads were used for the analysis (Fig. 1c), indicating that more RNA reads would generate a more accurate and exhaustive RNA editome, particularly for editing in the non-Alu region.

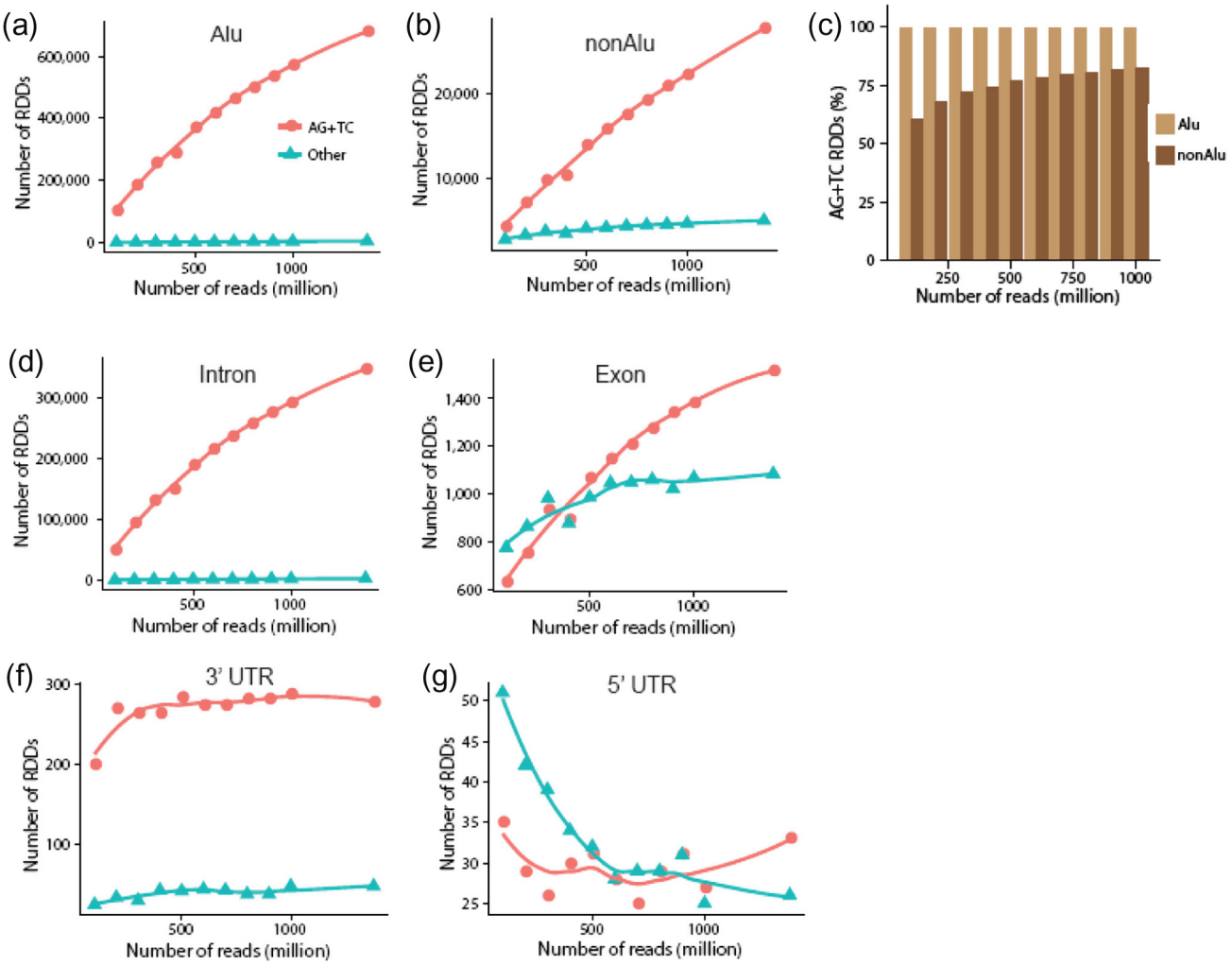

Fig. 1. (Color online) Influence of sequence coverage on detection of RNA editing. (a-b) influence of sequence coverage on the detection of RNA editing in the region of Alu and non-Alu. (c) ratio of A-to-G RDD detected using different numbers of sequenced reads. (d-g) influence of sequence coverage on the detection of RNA-editing in the exonic, intronic, 3′UTR and 5′ UTR regions.

Next, we investigated the influence of sequencing coverage on the editing sites at different genomic regions. More A-to-G/T-to-C RDDs were called in intronic and exonic regions when more reads were used (Fig. 1d, e). In contrast, in the 3′-UTR (untranslated region), only ~300 sites could be called with at least 200 million reads (Fig. 1f). The small number of editing sites detected in the 3′-UTR is incompatible with previous finding of many editing sites located in the 3′-UTR [42,43], which may be attributable to the low quality of UTR annotation in rhesus macaques due to limitations of bioinformatic methods in gene annotation with little transcriptome data. Similarly, in the 5′-UTR region, very few editing sites could be identified, but no significant increase was found when more reads were used (Fig. 1g). The ratios of other type of RDDs were comparatively lower in intronic and 3′-UTR regions but were relatively higher in exonic and 5′-UTR regions (Fig. 1d–g). The observation suggested that it is necessary to use large-scale sequenced RNA reads to accurately call RNA editing events in exonic and 5′-UTR regions.

3.2. A-to-I RNA editome of rhesus macaque

Considering that more transcriptomic data will be helpful to improve the identification of RNA editing sites, we used all transcriptomic data to identify RNA editing sites. With respect to the high false-positive rate of other types of RNA editing [44], we only considered A-to-I (G) RNA editing, which were A-to-G/T-to-C RDDs. A total of 707,246 A-to-I RNA editing sites were identified in the rhesus macaque (Fig. 2a, b). A high percentage of A-to-I RNA editing among all RDDs types (98.62%) implies that our method had a low false-discovery rate. To further confirm the accuracy of our datasets, we randomly chose 16 sites for validation by Sanger sequencing, and all of these sites turned out to be true (Fig. S2). Compared with the previous study, which identified only 31,250 RNA-editing sites [39], the number of editing sites detected in our study was unprecedented, likely due to the different filtering strategies employed, and more samples (30 samples including 21 from brain in this study versus 7 samples including 2 from brain from Ref. [39]), and large data size (1.96 billion reads in this study versus 824.8 millions reads in Ref. [39]).

A total of 310,888 A-to-I RNA editing sites within gene regions were used for the following analyses. Only 98,545 RNA editing sites were conserved between humans and rhesus macaques, highlighting rapid origin of RNA editing during evolution. As expected, conserved RNA editing sites displayed higher levels of RNA editing than nonconserved RNA editing and thus may possess more important functions (Fig. 2d).

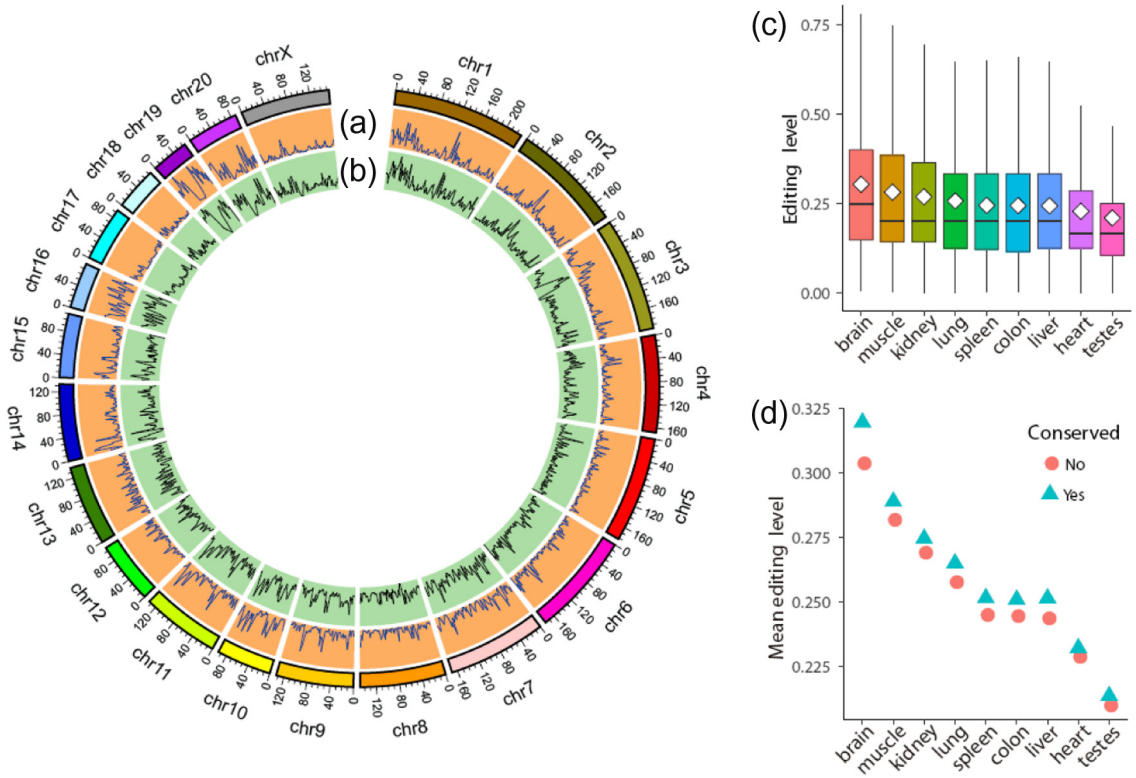

Fig. 2. (Color online) RNA editome of the genome of rhesus macaque. (a-b) Distribution of RNA editing in the genomes (a) and Alu regions (b) of a male rhesus macaque. (c) Editing level within different tissues. (d) Editing levels of RNA editing sites conserved and non-conserved between human and rhesus macaque within different tissues. The analyses in (c-d) were based on transcriptome data from different tissues including brain, colon, heart, kidney, liver, lung, skeletal muscle, spleen, and testes that were taken from the study by Merkin et al. [35].

3.3. Frequent occurrence of RNA editing in nuclear genes involved in mitochondrial function in primate

Editing level of each tissue was calculated as the average editing level of all RNA editing sites in the tissue. Comparison among different tissues revealed that the level of RNA editing was most pronounced in the brain, while testis harbored the lowest level of RNA editing (Fig. 2c and d).

When comparing editing levels among different tissues, we found that editing level were positively correlated with expression levels of *ADAR1* and *ADAR2*, but not *ADAR3*, among different tissues ($P < 0.05$, by Pearson correlation analysis, Fig. 3a–c). Editing level didn't exhibit correlation with sequence coverage (Fig. 3d). We sought to identify the sites where editing level was correlated with expression values of *ADAR* genes. However, the editing levels of only 1483, 1873, and 1498 sites were correlated with *ADAR1*, *ADAR2*, or *ADAR3* mRNA expression, respectively (Fig. S3a). This suggests that editing levels of many RNA editing sites in a tissue may not be dependent only on the mRNA expression of *ADAR* genes. Some other factors, like the splicing machinery, which also targets RNA, might influence double-stranded RNA strength and shape, and the editing level [30].

Annotation of these sites with editing levels correlating with mRNA expression of *ADAR1*, *ADAR2*, or *ADAR3* identified 756, 861, and 754 genes, respectively (Fig. S3b). Gene enrichment analyses of these genes showed that the categories associated with mitochondria were over-represented (Table S3). The finding indicated that many genes having function in mitochondria could be influenced by the *ADAR* genes. Inspired by the finding, we next investigated function of A-to-I RNA editing in nuclear genes involved in mitochondria.

3.4. Knock-down of ADAR affects mitochondria

To explore potential function of A-to-I RNA editing in mitochondria, we firstly depleted endogenous *ADAR1* or *ADAR2* expression in human glioma cell line U251 by RNA interference (Fig. 4, Fig. S4). The reduced protein expression levels of ADAR1 or ADAR2 were well confirmed with antibody. Cells transfected with negative control siRNA (scramble) and *ADAR1* siRNAs retained the normal tubular spiral mitochondrial network (Fig. S4a). In contrast, the mitochondria in cells transfected with *ADAR2* siRNAs frequently exhibited a highly interconnected, fibrous, and more elongated form (Fig. 4a). We further assessed the influence of knock down of ADAR1 and ADAR2 on the protein expression levels of ATP5A, TIM23, TOM20, MFN1, and COXIV, which are the key proteins involved in mitochondrial functions. Consequently, the expression of ATP5A, TIM23, and MFN1 were upregulated upon ADAR2 siRNAs transfection (Fig. 4b–f), and the expression of ATP5A was upregulated upon ADAR1 siRNAs transfection (Fig. S4d). ATP5A encodes a subunit of mitochondrial ATP synthase [45]. TIM23 is part of a complex located in the inner mitochondrial membrane that mediates the transport of transit peptide-containing proteins across the membrane [46]. MFN1 is a mediator of mitochondrial fusion [47]. The altered expression levels of these mitochondrial proteins in response to ADAR2 knockdown are consistent with the notion that ADAR genes play a key role in regulating mitochondrial function.

Similarly, the level of ATP production was upregulated after knockdown of ADAR1 (Fig. S4f) and ADAR2 (Fig. 4h). In contrast, the mitomass (mitochondrial mass) did not change (Fig. S4e, Fig. 4g) upon knockdown of the two *ADAR* genes. These experiments suggested that ADAR1 and ADAR2 have a functional impact on mitochondria and nuclear genes involved in mitochondria. The

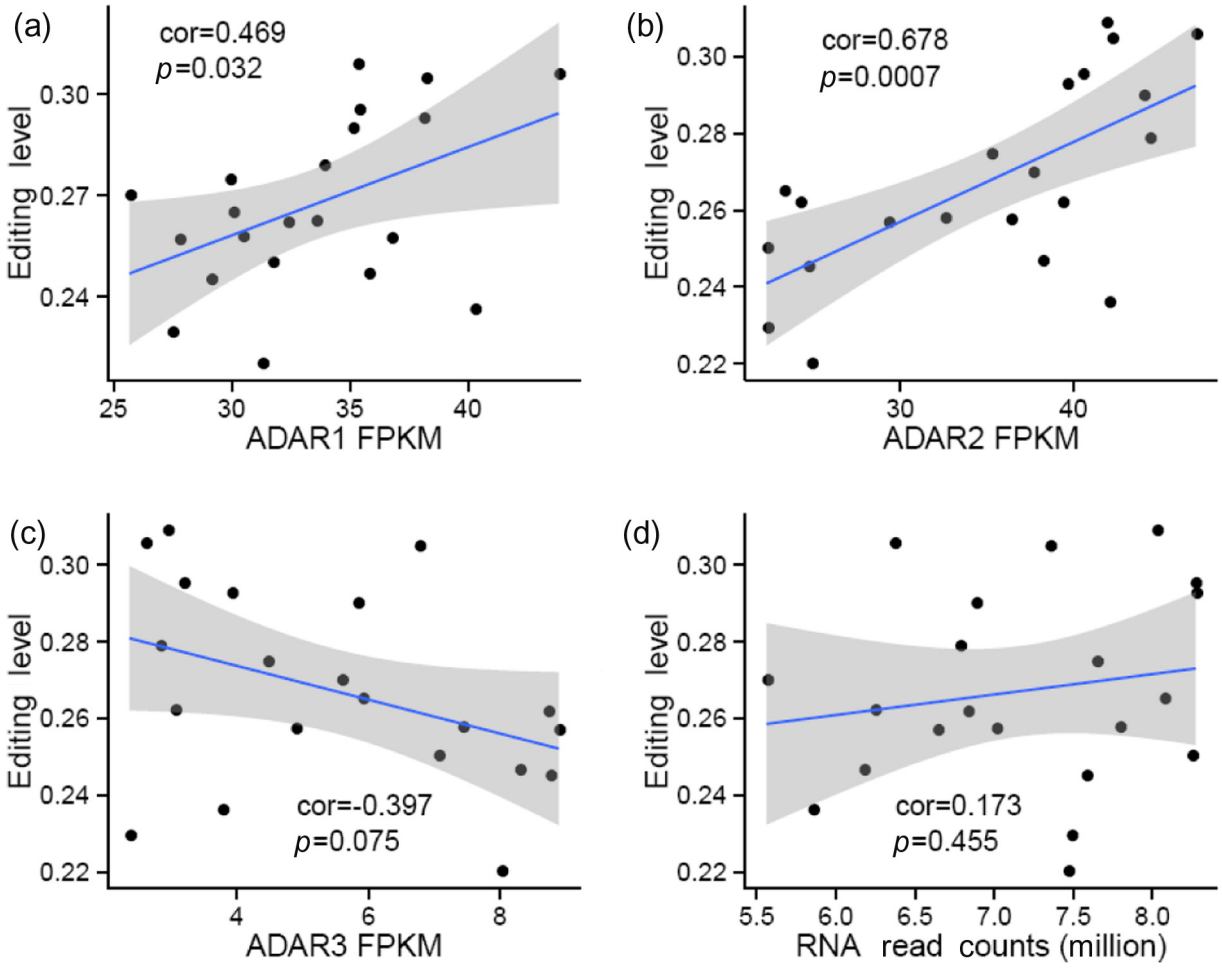

Fig. 3. (Color online) Correlation of editing levels with the mRNA expression levels of *ADAR*. Editing level of each tissue was calculated as the average editing level of all RNA editing sites in the tissue. Each dot in the figure represents a tissue. (a-b) Editing levels were positively correlated with the mRNA expression levels of *ADAR1* and *ADAR2* among different tissues. (c) No positive correlation was found between editing level and *ADAR3* mRNA expression level. (d) No positive correlation was found between editing level and sequence coverage of samples.

caveat of this experiment is that ADAR might function, not dependent of its editing activity [48]. Therefore, we could not conclude whether phenotypic changes in mitochondria were attributable to changes of RNA editing or changes of gene expression induced by ADAR, although ADAR is responsible for RNA editing.

3.5. Examining dynamics of RNA editing level during early development of the brain found an amino-acid-changing RNA editing site in MFN1, a mediator of mitochondrial fusion

Previous studies found that editing levels of RNA editing sites changed during the development of the mammalian brain [49–52]. Inspired by this observation, we investigated whether any RNA editing in genes involved in mitochondria might be coupled to the brain development. We leveraged transcriptomic data from the prefrontal cortex of 39 male macaques, with ages ranging from −56 days to 21 years, 8 days (minus indicates days before birth) (these data were first reported by He and coworkers [34]), to investigate editing dynamics during brain development. Based on the macaque editome retrieved above, we found that the editing levels increased dramatically in early age, while there was no significant alteration in adulthood (Fig. 5a and c). It corroborates that editing efficiency increases during neuronal differentiation and brain maturation [53].

We also examined the dynamics of expression values of *ADAR1*, *ADAR2*, and *ADAR3* genes, which are the three key genes encoding the enzyme responsible for A-to-I RNA editing by site-specific deamination of adenosines. The expression pattern of *ADAR1* and *ADAR2* mirrored the pattern of change observed in editing levels, with dramatic increases in the early stages of life (Fig. 5b, d, e), indicating that both *ADAR1* and *ADAR2* play important roles in brain development. In stark contrast, the expression level of *ADAR3* decreased during early brain development (Fig. 5b, f). In order to further validate the dramatic increase in RNA-editing level in early developmental stages observed in macaques, we repeated the editing dynamics analysis using human editing sites downloaded from Rigorously Annotated Database of A-to-I RNA Editing (RADAR) [33], plus the reported brain transcriptome data from 14 male adolescents [54]. As expected, a similar pattern was found during the early stages of human brain development (Fig. S5)).

Furthermore, we sought to identify the sites undergoing significant changes during brain development. In total, 172 sites with editing levels positively correlated with age were identified ($P < 0.05$), of which 162 sites were in introns, 5 in the 3′-UTR, and 5 in coding exons. The 172 sites were located in 102 genes, and gene enrichment analysis revealed two enriched terms: ionotropic glutamate receptor signaling pathway (gene ontology (GO): 0035235, genes *ATP1A3*, *GRIA2*, *GRIA3*, *GRIK1*) and glutamatergic synapse (KEGG: 04724) (*PLA2G4C*, *GNB4*, *GRIA2*, *GRIA3*, *GRIK1*)

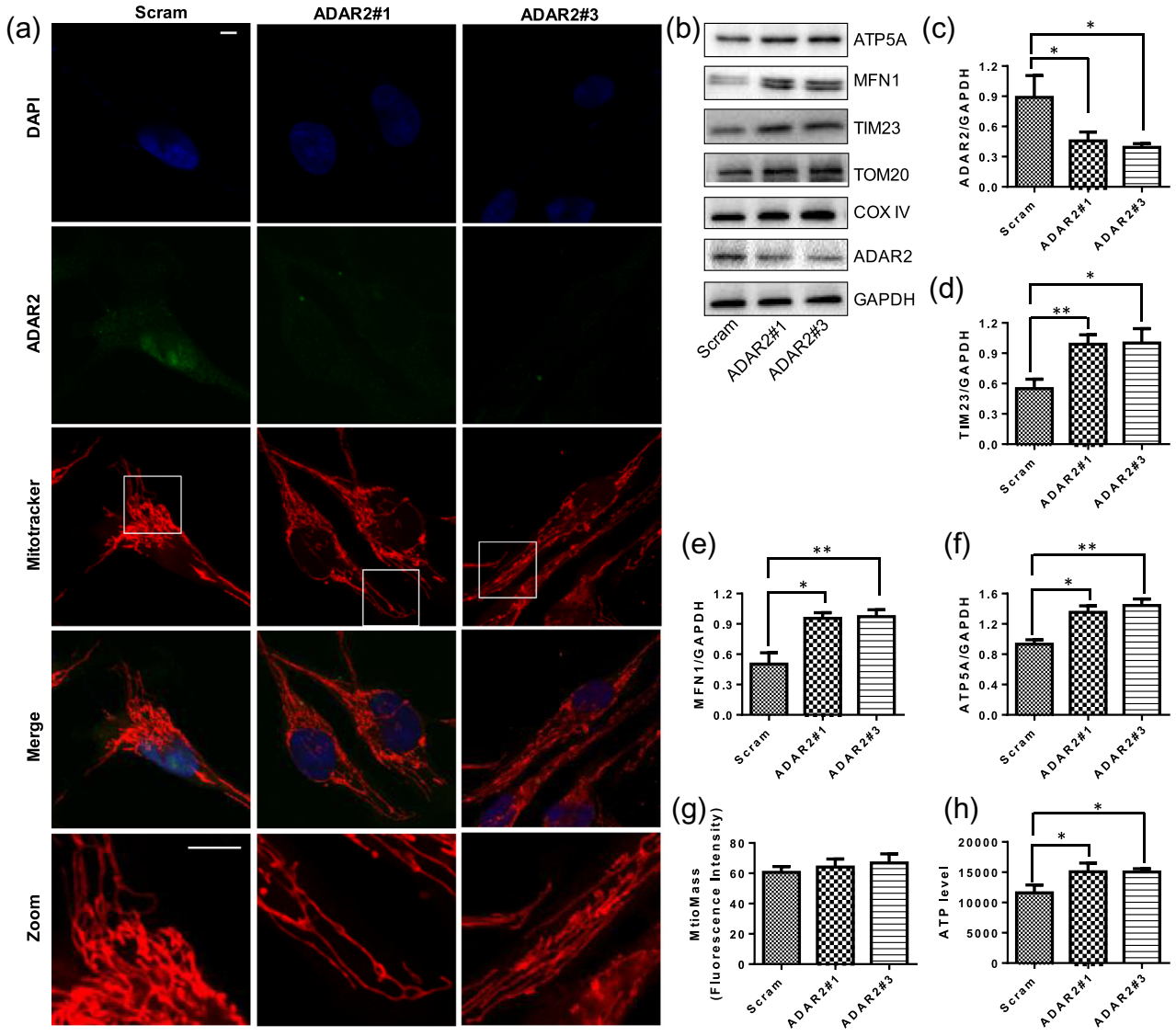

Fig. 4. (Color online) Effects of *ADAR2* knockdown on mitochondrial morphology and mitochondrial functions. (a) Influence on mitochondrial morphology after knocking down expression of *ADAR2*. Two siRNAs (ADAR2 and ADAR2) were used for specific knockdown of *ADAR2*. (b) Western blot of proteins involved in mitochondrial functions. (c-f) Changes in protein expression of ADAR2 (c), TIM23 (d), MFN1 (e) and ATP5A (f) after knockdown of *ADAR2*. ImageJ (National Institutes of Health, Bethesda, Maryland, USA) was used to quantify western blot bands in (b). (g) The mitomass did not change after knock down of *ADAR2*. (h) Increased ATP production level after knock down of *ADAR2*. Data were represented as mean ± SEM. Differences were analyzed by one-way analysis of variance (ANOVA). A *P*-value of <0.05 was considered to indicate a significant difference.

(Table S4, $P = 8.01 \times 10^{-3}$). Genes encoding the glutamate receptor channel have been reported to be regulated by editing [49,50]. The change in editing level implies that the glutamate receptor channel may experience functional regulatory modulation during brain development.

We then focused on four editing sites that cause non-synonymous changes in four genes: GRIK1 (Q638/R), GRIA2 (R717/G), KCNA1 (I400/V), and MFN1 (I234/V). As expected, all four sites harbored significantly higher editing levels in the brain (Fig. S6). GRIK1 Q/R editing level has been reported to increase during the development of the rat hippocampus [50], whereas the GRIA2 R/G editing level increased during the development of the rat embryonic brain and caused faster recovery from desensitization [49]. As for KCNA1 I/V, the editing was located in the pore-lining S6 domain of Shaker-type K^+ channels [9].

While MFN1 is known to be a mediator of mitochondrial fusion [47], no study has reported the functional consequence of MFN1 I234/V. Therefore, in this study, we first validated the editing site I234/V by Sanger sequencing (Fig. 6a). Then, guided by the findings from a previous study revealing that phosphorylation of MFN1 by ERK could regulate cell death and apoptosis in primary cortical neurons [55], we tested whether RNA editing of MFN1 (I234/V) altered its function. We constructed the expression vectors of pcDNA3-MFN1 and pcDNA3-MFN1 (I234/V) and transfected them into the human glioblastoma T98G cell line (Fig. 6b). The overexpression of unedited MFN1 and edited MFN1 proteins was confirmed by using both anti-myc (N-terminal tag) and anti-Flag (C-terminal tag) antibodies (Fig. 6c). Cell growth of unedited MFN1 and edited MFN1 (I234/V) overexpression was determined in T98G cells by the sulforhodamine B (SRB) assay [38]. The overex-

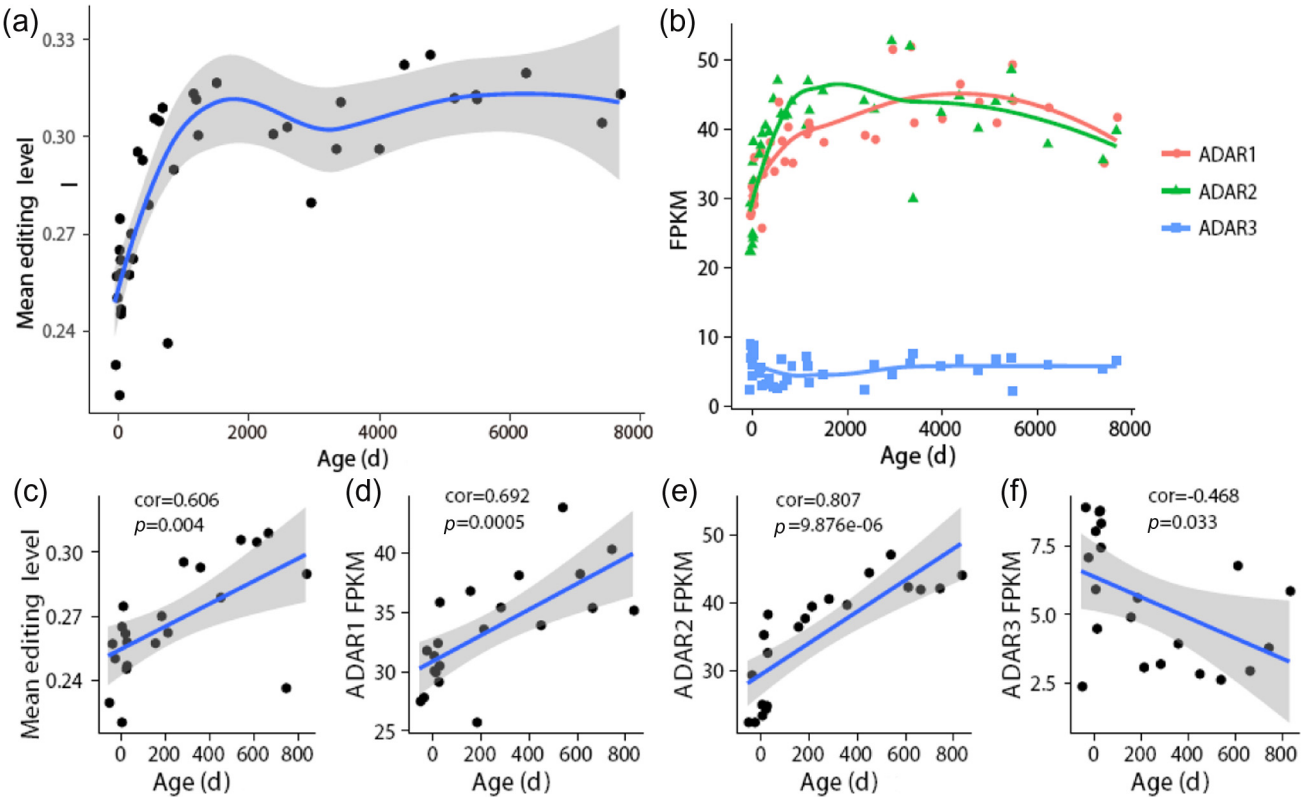

Fig. 5. Change in RNA Editing Level during Brain Development. (a-b) Change in RNA editing level (a) and expression of *ADAR* (b) during brain development. The analyses were based on transcriptomic data from the prefrontal cortex of 39 male macaques, with ages ranging from −56 days to 21 years, 8 days (minus indicate days before birth) from a previous study [34]. (c) Correlation between editing level and age. (d-f) Correlation between *ADAR* expression and age.

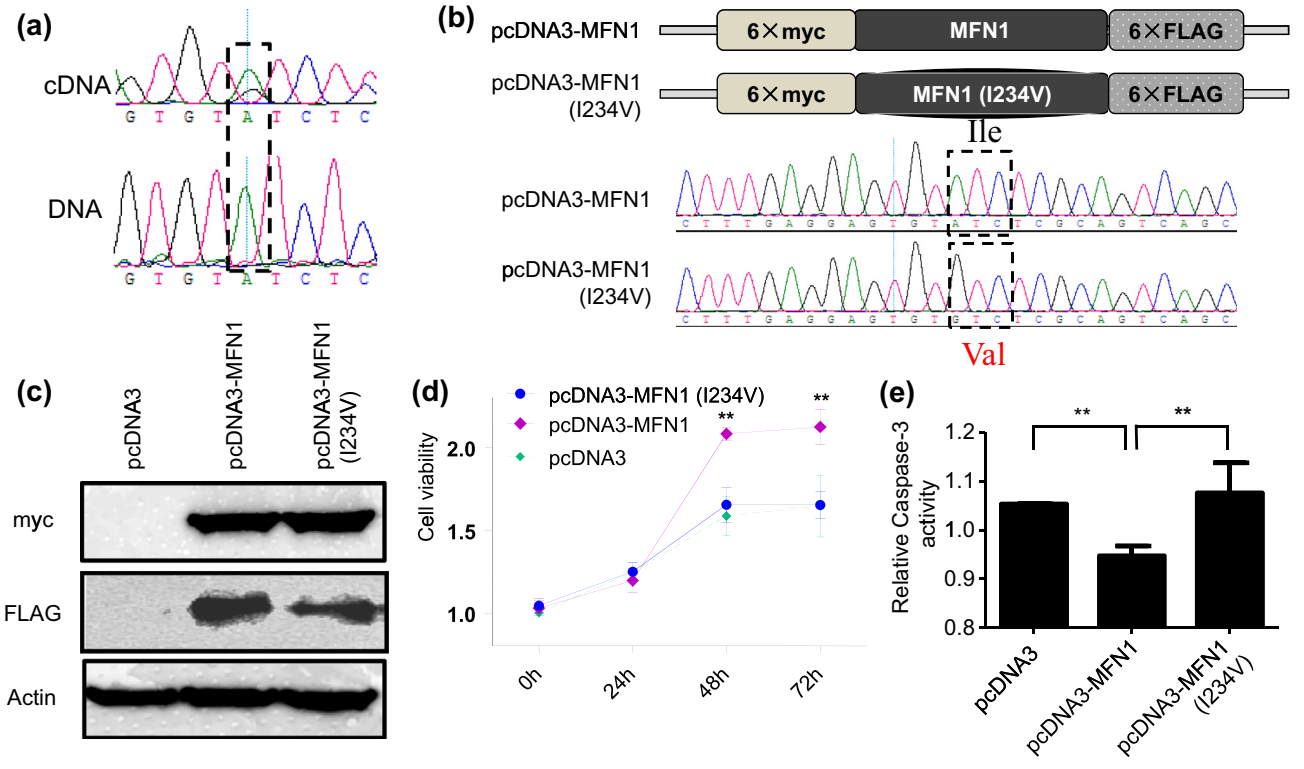

Fig. 6. Functional characterization of MFN1 RNA editing site (I234/V). (a) Validation of MFN1 RNA editing site (I234/V) by Sanger sequencing. (b) Schematic representation of expressional plasmids of MFN1 and its RNA editing MFN1 (I234/V). A 6×myc tag and a 6×Flag tag were attached to the N- and C-termini of target genes, respectively. The RNA editing site of MFN1 (I234) in the expression vector was confirmed by Sanger sequencing. (c) Identification of MFN1 and MFN1 (I234/V) overexpression in T98G cells. The overexpression of MFN1 and MFN1 (I234/V) was detected using either anti-myc or anti-FLAG antibody. (d) Cell growth of MFN1 and MFN1 (I234/V) overexpression was determined in T98G cells by the SRB assay. (e) Quantification of apoptosis in MFN1 and MFN1 (I234/V) overexpression cells at 48 h. $^{**}P < 0.001$. All functional experiments were performed in triplicate and repeated for three times.

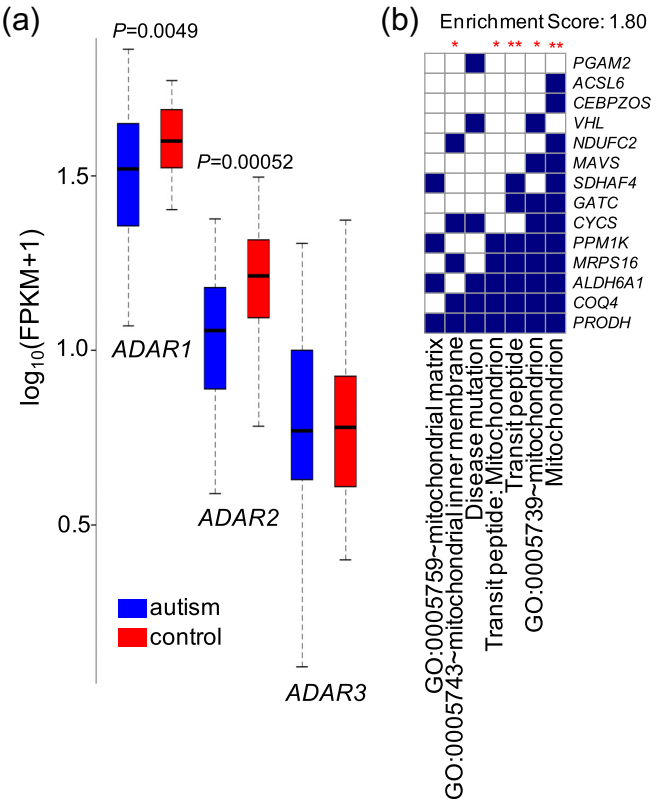

Fig. 7. Dysregulation of RNA editing in nuclear genes involved in mitochondria in autism. (a) Expression level of *ADAR* genes in prefrontal cortex of autism and control. The original data of 34 autism cases (2–60 years old) and 40 controls (0–62 years old) were taken from a previous study by Liu et al. [37]. (b) Gene enrichment analysis by DAVID program (https://david.ncifcrf.gov/) found that 14 genes at 7 categories were associated with mitochondria. Blue color indicated corresponding gene-term association positively reported. $^{**}P < 0.01$ and $^{*}P < 0.05$.

pression of MFN1 dramatically increased cell proliferation at 48 h and 72 h after transfection. However, overexpression of edited MFN1 (I234/V) significantly suppressed cell proliferation compared with unedited MFN1 overexpression at 48 h ($P < 0.001$) and 72 h ($P < 0.001$) (Fig. 6d). In addition, overexpression of unedited MFN1 significantly suppressed apoptosis compared with empty vector ($P < 0.001$), but I234/V editing resulted a decrease in suppressing apoptosis ($P < 0.001$) (Fig. 6e). These results suggest that MFN1 I234/V editing has a functional consequence.

3.6. Examining brain disorder found dys-regulation of RNA editing in nuclear genes involved in mitochondria in autism

The most important impact of A-to-I RNA editing pertains to the nervous system [3,8–10]. Dysregulation of RNA editing can induce a variety of diseases of the nervous system [11–14]. We examined whether any gene involved in mitochondria harboring dysregulated RNA editing in autism spectrum disorder (ASD), which is a group of clinically heterogeneous neurodevelopmental disorders characterized by the disruption of social functioning and inclination toward restricted interests and repetitive behaviors [56,57]. By comparing the prefrontal cortex transcriptomes of 34 autism cases (2–60 y old) and 40 controls (0–62 y old) [37], we found that expression levels of *ADAR1* and *ADAR2* were down-regulated in autism (Fig. 7a, $P = 0.0049$ and 0.00052, respectively, based on linear model), suggesting potential change of RNA editing in autism. Totally 75 sites located within 57 genes were identified to exhibit significantly differential editing levels between autism and control (Table S5). Gene enrichment analysis of these genes found 14 genes involved in mitochondria (Fig. 7b, Table S6). This finding of an association supported function of nuclear gene RNA editing in mitochondria, although more experiments were needed to validate functional consequence of these RNA editing sites.

4. Discussion

The rhesus macaque (*Macaca mulatta*), which is physiologically and anatomically close to humans and responds similarly to many diseases, provides a huge advantage over other animal models [58,59]. It will be necessary to study some primate-specific mechanisms or diseases in the rhesus macaque because the same research in humans could not be performed due to ethical issue. There have been many studies using the rhesus macaque as an animal model to study brain evolution [34,60], specific virus invasion [61], embryonic stem cells [36] (for a review, Ref [59]). Expansion of RNA editing in primate made rhesus macaque as perfect model to study function of RNA editing. In this study, we constructed the primate editome of *Macaca mulatta* and characterized the functions of RNA editing in mitochondria.

4.1. RNA editing occurring in nuclear genes influence the function of mitochondria

Although RNA editing has frequently been observed in mitochondrial sequences, most frequent are C-to-U types [62]. Whether A-to-I RNA editing has functions in nuclear genes involved in mitochondria remains elusive. Here, we found that A-to-I RNA editing occurred frequently in nuclear genes that have functions in mitochondria. When knocking down the expression of *ADAR1* and *ADAR2*, which are the key genes encoding the enzyme responsible for RNA editing, the mitochondrial structure, the level of ATP production, and the protein expression of some key genes involved in mitochondrial function, were changed. These data suggested that RNA editing might have a significant function in mitochondria via their influence on nuclear-coded mitochondrial genes.

4.2. RNA editing during early stages of brain development

After birth, neurogenesis proceeds with rapid generation of glial cells until early childhood. Brain development in the early postnatal stage is characterized by an enormous proliferation of dendrites and axons and subsequent synaptogenesis, glial proliferation, and myelination, mainly in the forebrain and cerebellum [63]. From late childhood to adolescence, considerable structural modifications and molecular reorganization of neural circuits continue, although in a less dramatic fashion compared with the initial prenatal and early postnatal stages. These later developmental changes coincide with the emergence of higher-order cognition and complex behavior [63]. Although the causal relationship between a dramatic increase in the level of RNA editing and brain development is unclear, evidence suggests that RNA editing might be key in neurogenesis, and as neurogenesis proceeds, RNA editing levels consequently increase [53]. Indeed, the editing level increased during the process of differentiation of embryonic stem cells to neural stem cells (Fig. S7). Our analysis for the dynamics of RNA editing level during early development of the brain identified an amino-acid-changing RNA editing site in MFN1, a well known mediator of mitochondrial fusion [47]. Further functional assays at the cellular level, using this particular case, showed the RNA editing site in MFN1 affected cell proliferation and apoptosis (Fig. 7), which provided evidence to support an active role of RNA editing in brain development.

In conclusion, our extensive investigation of primate editome supported that A-to-I RNA editing had a role in mitochondria by influencing nuclear genes involved in the function of mitochondria based on the following lines of evidences: (1) frequent occurrence of RNA editing in many nuclear genes involved in mitochondria; (2) RNA editing site in *MFN1*, a mediator of mitochondrial fusion, is associated with brain development; (3) dys-regulation of RNA editing in nuclear genes involved in mitochondria in autism; (4) knock-down of *ADAR* affects mitochondrial phenotypes. These data will lay a basis for further characterization of RNA editing pattern in brain development and brain diseases.

Conflict of interest

The authors declare that they have no conflict of interest.

Author contributions

D.D.W., Y.G.Y., and Y. P. Z. led and designed the project. L.Q.Y. and X.D.R. performed data analysis of RNA editing. H.Z. and L.L.L. performed the MFN1 editing experiment. H.J.Z. performed the related experiments in cells with knockdown of ADAR1 and ADAR2. Z.B.W. and X.T.H. dissected the rhesus macaque tissues. M.M.Y. performed the Sanger sequencing experiment. L.Z. performed genomic analysis from each tissue. L.Q.Y. and D.D.W. drafted the manuscript with input from the other authors. All authors read, commented on, and improved the manuscript.

Acknowledgments

This work was supported by the Strategic Priority Research Program of the Chinese Academy of Sciences (XDB13020600) and the National Natural Science Foundation of China (31671325).

Appendix A. Supplementary data

Supplementary data associated with this article can be found, in the online version, at http://dx.doi.org/10.1016/j.scib.2017.05.021.

References

[1] Bass BL. RNA editing by adenosine deaminases that act on RNA. Annu Rev Biochem 2002;71:817–46.
[2] Nishikura K. Functions and regulation of RNA editing by ADAR deaminases. Annu Rev Biochem 2010;79:321–49.
[3] Li JB. Church GM Deciphering the functions and regulation of brain-enriched A-to-I RNA editing. Nat Neurosci 2013;16:1518–22.
[4] Wang Q, Khillan J, Gadue P, et al. Requirement of the RNA editing deaminase ADAR1 gene for embryonic erythropoiesis. Science 2000;290:1765–8.
[5] Higuchi M, Maas S, Single FN, et al. Point mutation in an AMPA receptor gene rescues lethality in mice deficient in the RNA-editing enzyme ADAR2. Nature 2000;406:78–81.
[6] Palladino MJ, Keegan LP, O'Connell MA, et al. A-to-I pre-mRNA editing in drosophila is primarily involved in adult nervous system function and integrity. Cell 2000;102:437–49.
[7] Tonkin LA, Saccomanno L, Morse DP, et al. RNA editing by ADARs is important for normal behavior in Caenorhabditis elegans. EMBO J 2002;21:6025–35.
[8] Seeburg PH. Hartner J Regulation of ion channel/neurotransmitter receptor function by RNA editing. Curr Opin Neurobio 2003;13:279–83.
[9] Hoopengardner B, Bhalla T, Staber C, et al. Nervous system targets of RNA editing identified by comparative genomics. Science 2003;301:832–6.
[10] Hwang T, Park C-K, Leung AKL, et al. Dynamic regulation of RNA editing in human brain development and disease. Nat Neurosci 2016;19:1093–9.
[11] Maas S, Kawahara Y, Tamburro KM, et al. A-to-I RNA editing and human disease. RNA Biol 2006;3:1–9.
[12] Eran A, Li JB, Vatalaro K, et al. Comparative RNA editing in autistic and neurotypical cerebella. Mol Psychiatry 2013;18:1041–8.
[13] Khermesh K, D'Erchia AM, Barak M, et al. Reduced levels of protein recoding by A-to-I RNA editing in Alzheimer's disease. RNA 2016;22:290–302.
[14] Silberberg G, Lundin D, Navon R, et al. Deregulation of the A-to-I RNA editing mechanism in psychiatric disorders. Hum Mol Genet 2012;21:311–21.
[15] Gardiner K, Du Y. A-to-I editing of the 5HT2C receptor and behaviour. Brief Funct Genomic Proteomic 2006;5:37–42.
[16] Qi L, Chan THM, Tenen DG, et al. RNA editome imbalance in hepatocellular carcinoma. Cancer Res 2014;74:1301–6.
[17] Han L, Diao L, Yu S, et al. The genomic landscape and clinical relevance of A-to-I RNA editing in human cancers. Cancer Cell 2015;28:515–28.
[18] Paz-Yaacov N, Bazak L, Buchumenski I, et al. Elevated RNA editing activity is a major contributor to transcriptomic diversity in tumors. Cell Rep 2015;13:267–76.
[19] Fumagalli D, Gacquer D, Rothe F, et al. Principles governing A-to-I RNA editing in the breast cancer transcriptome. Cell Rep 2015;13:277–89.
[20] Qin Y-R, Qiao J-J, Chan THM, et al. Adenosine-to-Inosine RNA editing mediated by ADARs in esophageal squamous cell carcinoma. Cancer Res 2014;74:840–51.
[21] Liddicoat BJ, Chalk AM, Walkley CR. ADAR1, inosine and the immune sensing system: distinguishing self from non-self. Wiley Interdiscip Rev RNA 2016;7:157–72.
[22] Liddicoat BJ, Piskol R, Chalk AM, et al. RNA editing by ADAR1 prevents MDA5 sensing of endogenous dsRNA as nonself. Science 2015;349:1115–20.
[23] Mannion NM, Greenwood SM, Young R, et al. The RNA-editing enzyme ADAR1 controls innate immune responses to RNA. Cell Rep 2014;9:1482–94.
[24] Benne R, Van Den Burg J, Brakenhoff JPJ, et al. Major transcript of the frameshifted coxll gene from trypanosome mitochondria contains four nucleotides that are not encoded in the DNA. Cell 1986;46:819–26.
[25] Grewe F, Herres S, Viehover P, et al. A unique transcriptome: 1782 positions of RNA editing alter 1406 codon identities in mitochondrial mRNAs of the lycophyte Isoetes engelmannii. Nucl Acids Res 2010;39:2890–902.
[26] Rudinger M, Fritz-Laylin L, Polsakiewicz M, et al. Plant-type mitochondrial RNA editing in the protist *naegleria gruberi*. RNA 2011;17:2058–62.
[27] Fu C-J, Sheikh S, Miao W, et al. Missing genes, multiple ORFs, and C-to-U type RNA editing in *acrasis kona* (Heterolobosea, Excavata) mitochondrial DNA. Genome Biol Evol 2014;6:2240–57.
[28] Burger G, Yan Y, Javadi P, et al. Group I-intron trans-splicing and mRNA editing in the mitochondria of placozoan animals. Trends Genet 2009;25:381–6.
[29] Janke A, Paabo S. Editing of a tRNA anticodon in marsupial mitochondria changes its codon recognition. Nucl Acids Res 1993;21:1523–5.
[30] Wu DD, Ye LQ, Li Y, et al. Integrative analyses of RNA editing, alternative splicing, and expression of young genes in human brain transcriptome by deep RNA sequencing. J Mol Cell Biol 2015;7:314–25.
[31] Ramaswami G, Lin W, Piskol R, et al. Accurate identification of human Alu and non-Alu RNA editing sites. Nat Methods 2012;9:579–81.
[32] Ramaswami G, Zhang R, Piskol R, et al. Identifying RNA editing sites using RNA sequencing data alone. Nat Methods 2013;10:128–32.
[33] Ramaswami G, Li JB. RADAR: a rigorously annotated database of A-to-I RNA editing. Nucleic Acids Res 2014;42:D109–113.
[34] He Z, Bammann H, Han D, et al. Conserved expression of lincRNA during human and macaque prefrontal cortex development and maturation. RNA 2014;20:1103–11.
[35] Merkin J, Russell C, Chen P, et al. Evolutionary dynamics of gene and isoform regulation in mammalian tissues. Science 2012;338:1593–9.
[36] Zhao Y, Ji S, Wang J, et al. MRNA-Seq and microRNA-Seq whole-transcriptome analyses of rhesus monkey embryonic stem cell neural differentiation revealed the potential regulators of rosette neural stem cells. DNA Res 2014;21:541–54.
[37] Liu X, Han D, Somel M, et al. Disruption of an evolutionarily novel synaptic expression pattern in autism. PLoS Biol 2016;14:e1002558.
[38] Kong Y, Li F, Nian Y, et al. KHF16 is a leading structure from cimicifuga foetida that suppresses breast cancer partially by inhibiting the NF-κB signaling pathway. Theranostics 2016;6:875–86.
[39] Chen JY, Peng Z, Zhang R, et al. RNA editome in rhesus macaque shaped by purifying selection. PLoS Genet 2014;10. e1004274.
[40] Chen L. Characterization and comparison of human nuclear and cytosolic editomes. Proc Natl Acad Sci USA 2013;110:E2741–2747.
[41] Bazak L, Haviv A, Barak M, et al. A-to-I RNA editing occurs at over a hundred million genomic sites, located in a majority of human genes. Genome Res 2014;24:365–76.
[42] Gu T, Buaas FW, Simons AK, et al. Canonical A-to-I and C-to-U RNA editing Is enriched at 3'UTRs and microRNA target sites in multiple mouse tissues. PLoS One 2012;7:e33720.
[43] Li Q, Wang Z, Lian J, et al. Caste-specific RNA editomes in the leaf-cutting ant Acromyrmex echimatior. Nat Commun 2014;5:4943.
[44] Piskol R, Peng Z, Wang J, et al. Lack of evidence for existence of noncanonical RNA editing. Nat Biotechnol 2013;31:19–20.
[45] Akiyama S, Endo H, Inohara N, et al. Gene structure and cell type-specific expression of the human ATP synthase α subunit. Biochim Biophys Acta 1994;1219:129–40.
[46] Bauer MF, Gempel K, Reichert AS, et al. Genetic and structural characterization of the human mitochondrial inner membrane translocase1. J Mol Biol 1999;289:69–82.
[47] Chen H, Detmer SA, Ewald AJ, et al. Mitofusins Mfn1 and Mfn2 coordinately regulate mitochondrial fusion and are essential for embryonic development. J Cell Biol 2003;160:189–200.
[48] Chen T, Xiang J-F, Zhu S, et al. ADAR1 is required for differentiation and neural induction by regulating microRNA processing in a catalytically independent manner. Cell Res 2015;25:459–76.
[49] Seeburg PH, Higuchi M, Sprengel R. RNA editing of brain glutamate receptor channels: mechanism and physiology. Brain Res Brain Res Rev 1998;26:217–29.

[50] Bernard A, Ferhat L, Dessi F, et al. Q/R editing of the rat GluR5 and GluR6 kainate receptors in vivo and in vitro: evidence for independent developmental, pathological and cellular regulation. Eur J Neurosci 1999;11:604–16.
[51] Li Z, Bammann H, Li M, et al. Evolutionary and ontogenetic changes in RNA editing in human, chimpanzee, and macaque brains. RNA 2013;19:1693–702.
[52] Ekdahl Y, Farahani HS, Behm M, et al. A-to-I editing of microRNAs in the mammalian brain increases during development. Genome Res 2012;22:1477–87.
[53] Behm M, Öhman M. RNA editing: a contributor to neuronal dynamics in the mammalian brain. Trends Genet 2016;32:165–75.
[54] Plant TM, Ramaswamy S. Kisspeptin and the regulation of the hypothalamic-pituitary-gonadal axis in the rhesus monkey (Macaca mulatta). Peptides 2009;30:67–75.
[55] Pyakurel A, Savoia C, Hess D, et al. Extracellular regulated kinase phosphorylates mitofusin 1 to control mitochondrial morphology and apoptosis. Mol Cell 2015;58:244–54.
[56] Bourgeron T. From the genetic architecture to synaptic plasticity in autism spectrum disorder. Nat Rev Neurosci 2015;16:551–63.
[57] Geschwind DH, State MW. Gene hunting in autism spectrum disorder: on the path to precision medicine. Lancet Neurol 2015;14:1109–20.
[58] Pena JC. Monkey models of tuberculosis: lessons learned. Infect Immun 2015;83:852–62.
[59] Zhang X-L, Pang W, Hu X-T, et al. Experimental primates and non-human primate (NHP) models of human diseases in China: current status and progress. Zool Res 2014;35:447–64.
[60] Belmonte JCI, Callaway EM, Caddick SJ, et al. Brains, genes, and primates. Neuron 2015;86:617–31.
[61] Sandler NG, Bosinger SE, Estes JD, et al. Type I interferon responses in rhesus macaques prevent SIV infection and slow disease progression. Nature 2014;511:601–5.
[62] Moreira S, Valach M, Aoulad-Aissa M, et al. Novel modes of RNA editing in mitochondria. Nucleic Acids Res 2016;44:4907–19.
[63] Silbereis JC, Pochareddy S, Zhu Y, et al. The Cellular and molecular landscapes of the developing human central nervous system. Neuron 2016;89:248–68.

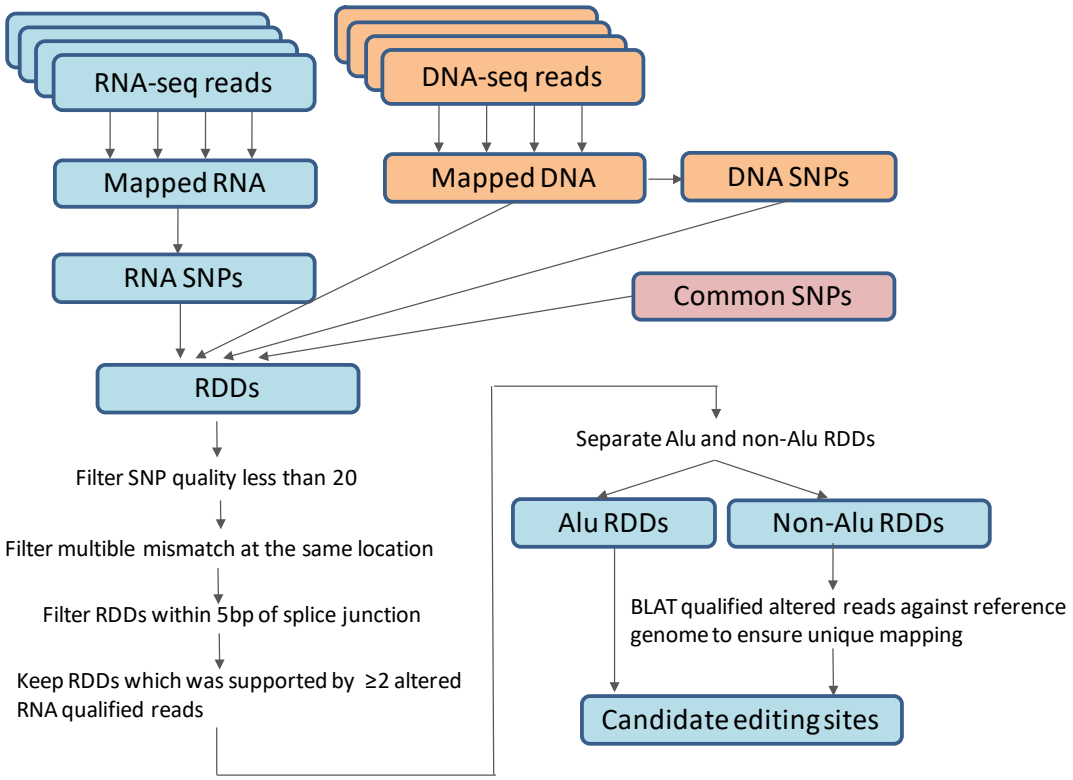

Figure S1. Pipeline used to call RNA editing in this study.

Enseml ID	Chrom	Positon	DNA Sequencing	RNA Sequencing
ENSMMUG00000009671	X	74686223	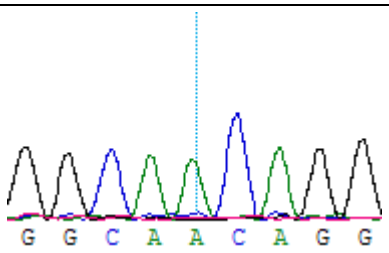	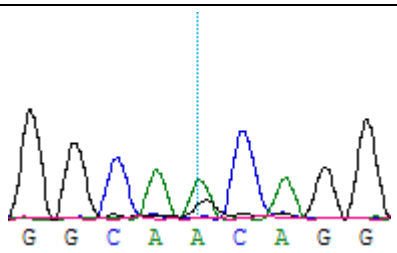
ENSMMUG00000016837	1	9077947	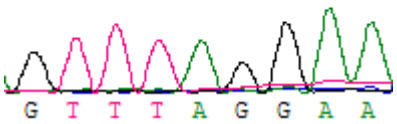	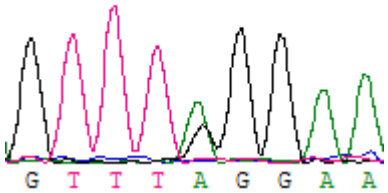
ENSMMUG00000016837	1	9078019	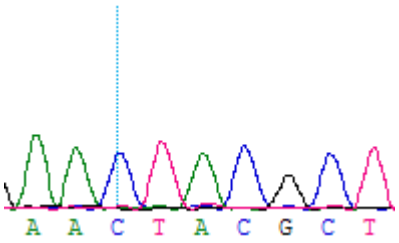	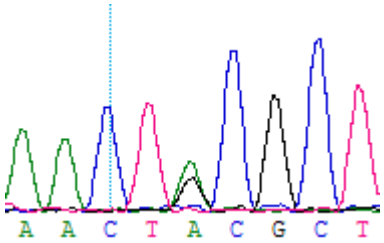
ENSMMUG00000018955	2	102382932	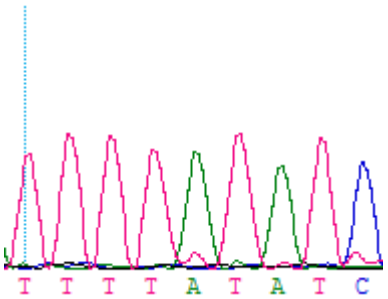	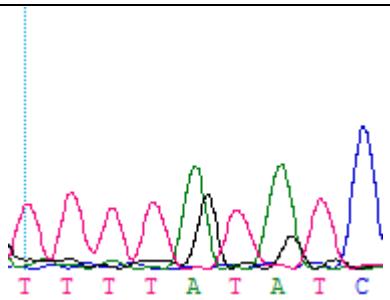
ENSMMUG00000006871	5	31070400	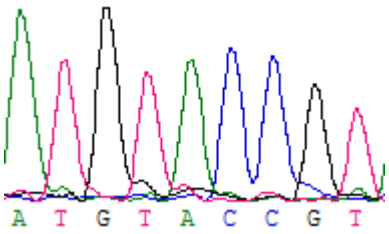	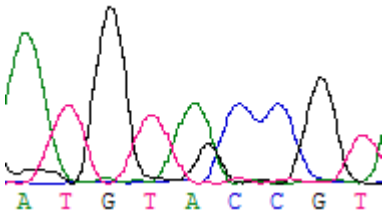
ENSMMUG00000006871	5	31070425	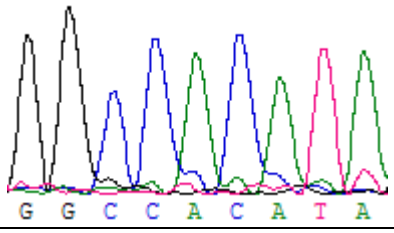	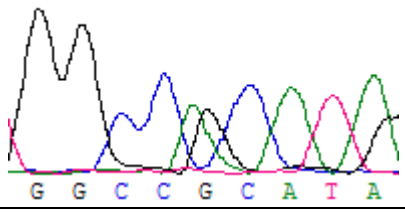

ENSMMUG00000023419	6	11241716	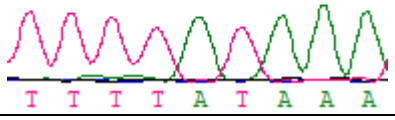	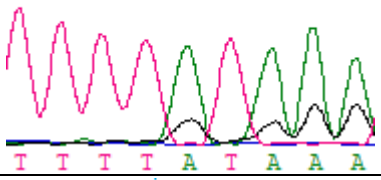
ENSMMUG00000023419	6	11242005	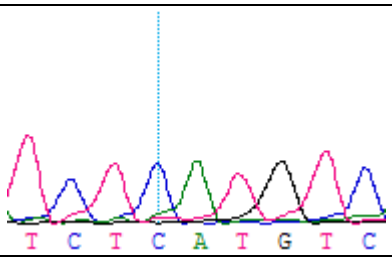	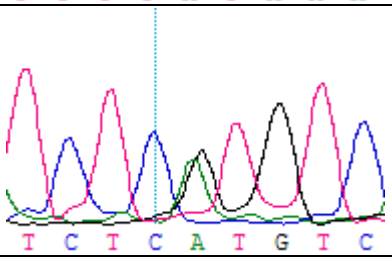
ENSMMUG00000021994	8	22580917	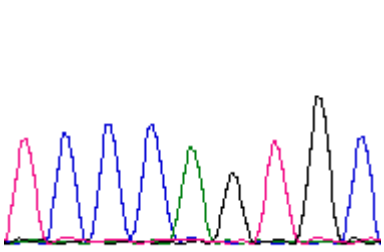	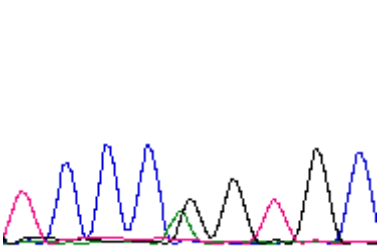
ENSMMUG00000021994	8	22580947	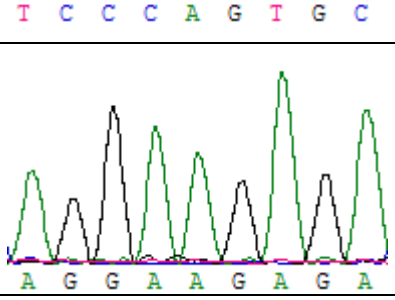	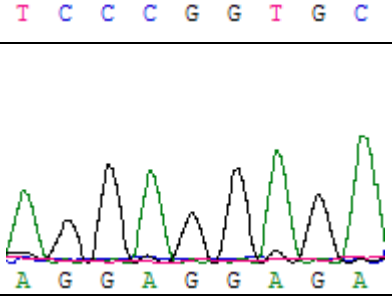
ENSMMUG00000010827	9	99885387	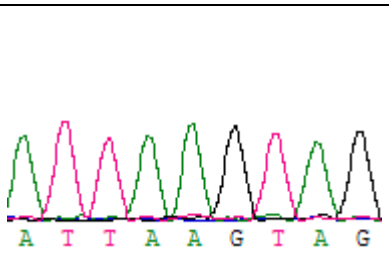	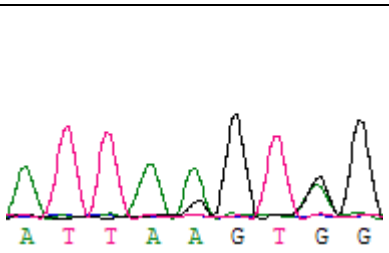
ENSMMUG00000010827	9	99885451	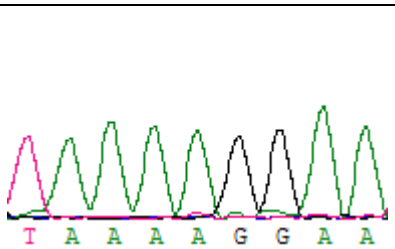	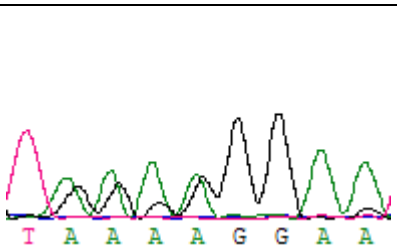
ENSMMUG00000020712	10	567182	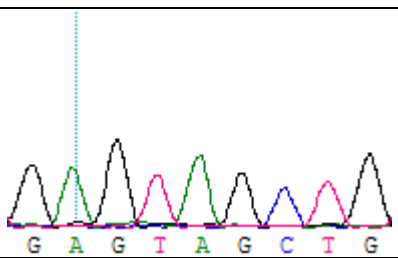	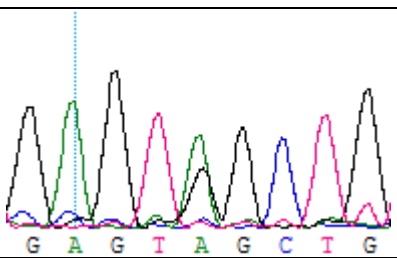

ENSMMUG00000020712	10	576358	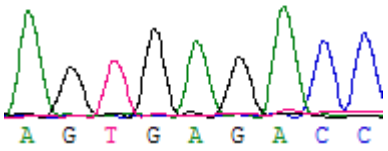	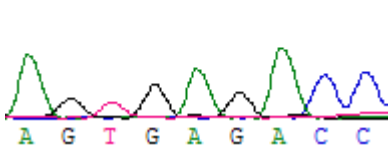
ENSMMUG00000015737	X	13069254	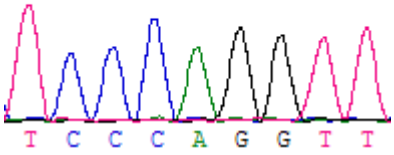	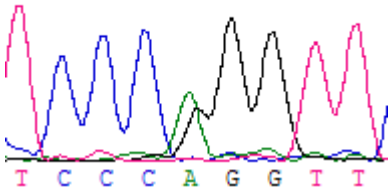
ENSMMUG00000015737	X	13069283	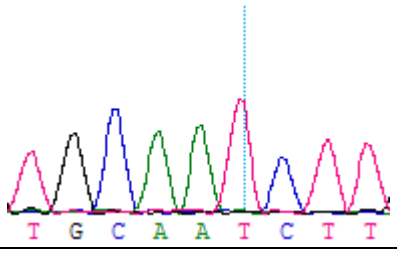	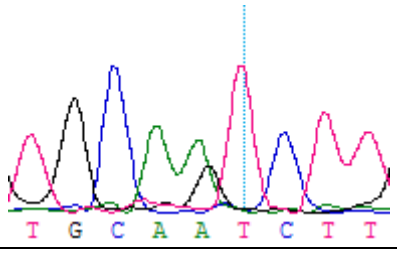

Figure S2. Validation of 16 RNA editing sites using Sanger sequencing

Chrom – Chromosome. The editing are the fifth bases from the left.

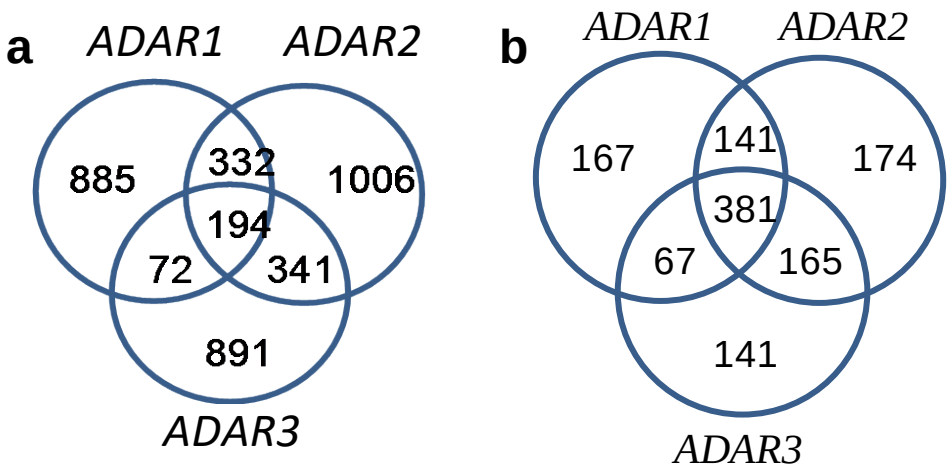

Figure S3. Number of sites (a) and genes (b) with editing levels that were associated with the mRNA expression of the *ADAR* genes.

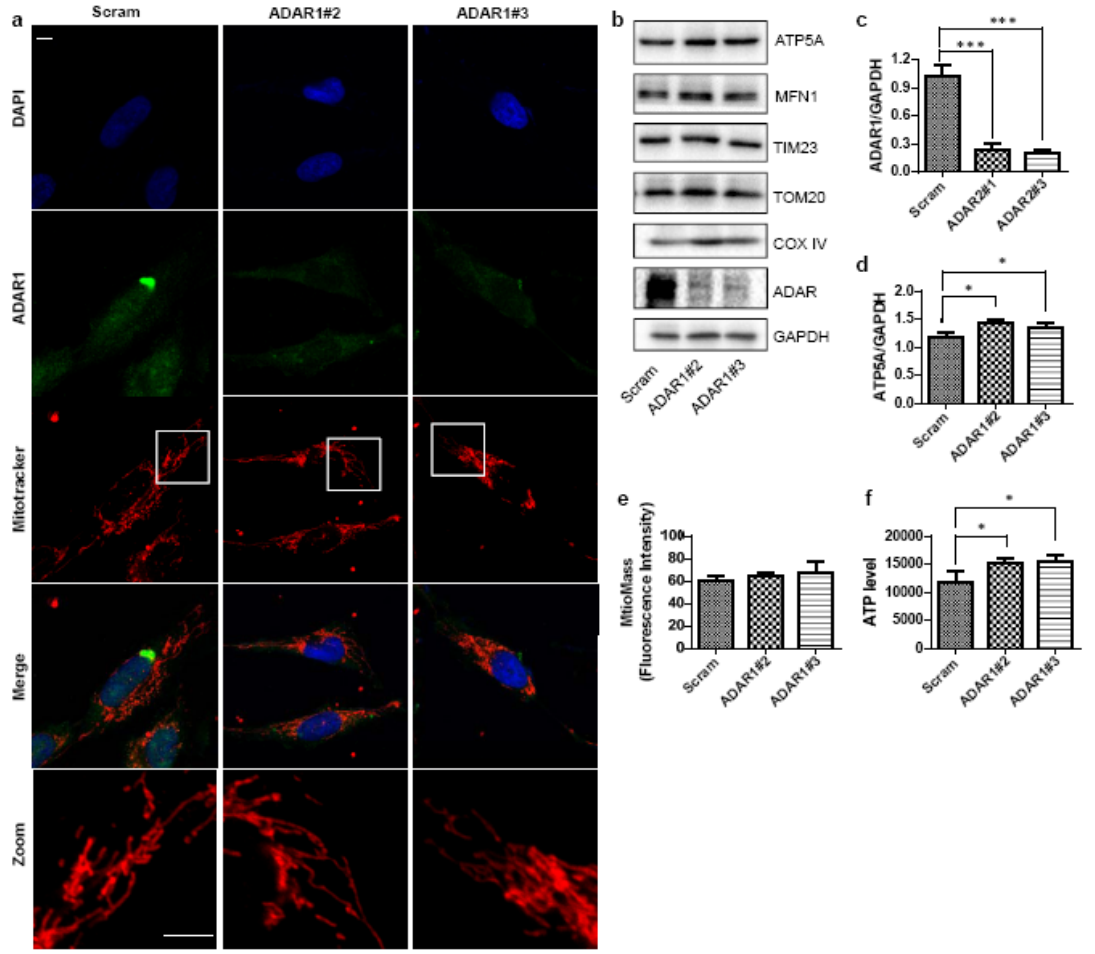

Figure S4. Effect of *ADAR1* knockdown on mitochondria. (a) No influence on mitochondrial morphology after knocking down expression of ADAR1. Two siRNAs (siRNA#2 and siRNA#3) were used for specific knockdown of *ADAR1*. (b) Western blot of proteins involved in mitochondrial functions. Change of ADAR1 (c) and ATP5A protein expression (d) after knockdown of *ADAR1*. ImageJ (National Institutes of Health, Bethesda, Maryland, USA) was used to quantify western blot bands in (b). (e) The mitomass did not change after knock down of ADAR1. (f) Increased ATP production level after knock down of ADAR1. Data were represented as mean ± SEM. Differences were analyzed by one-way analysis of variance (ANOVA). A P- value of <0.05 was considered to indicate a significant difference.

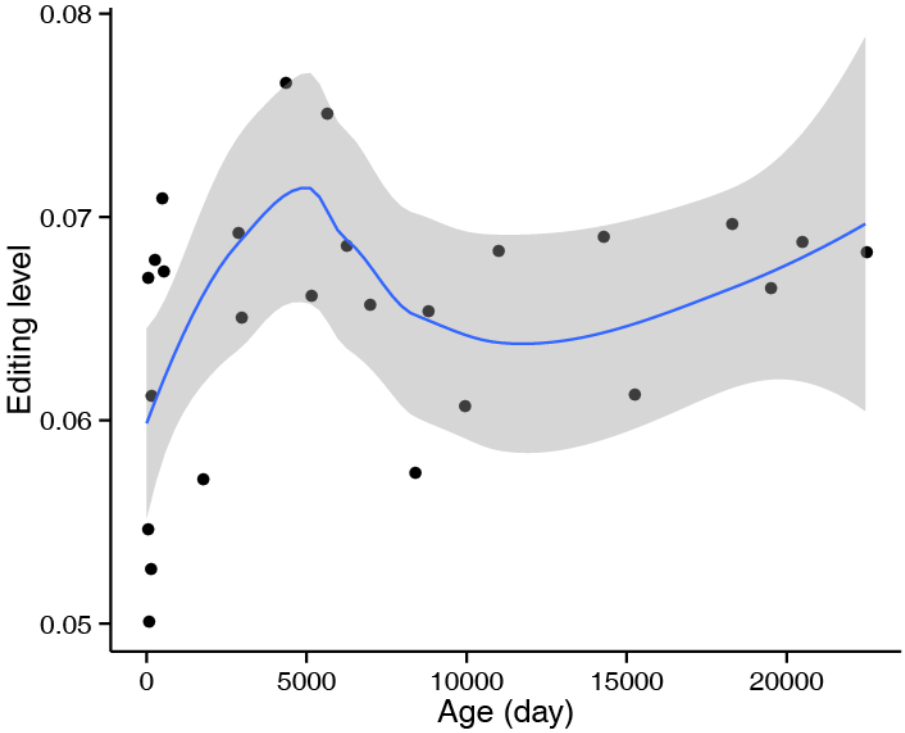

Figure S5. Change in RNA editing level during human brain development. Editing level of each tissue was calculated as the average editing level of all RNA editing sites in the tissue. Each dot in the figure represents a tissue.

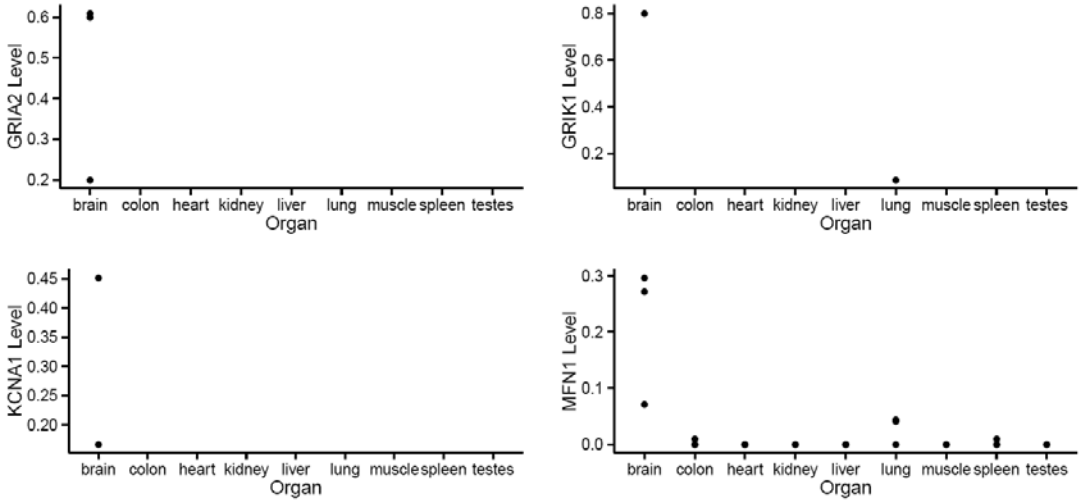

Figure S6. Editing level of the four editing sites GRIK1 (Q638/R), GRIA2 (R717/G), KCNA1 (I400/V), and MFN1 (I234V) among different tissues (Merkin et al 2012).

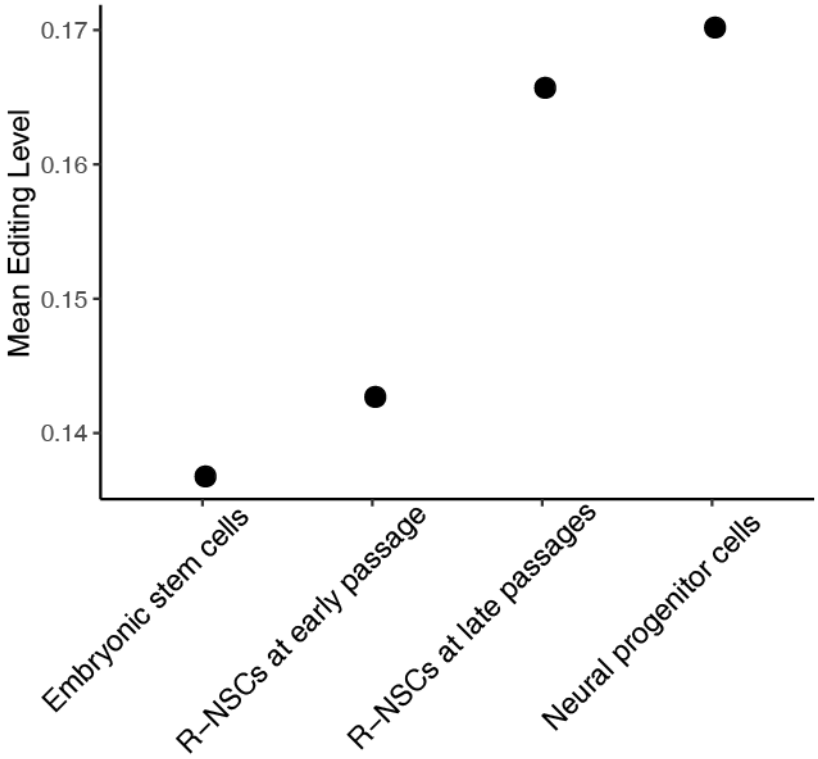

Figure S7. Dynamic changes of RNA editing level during the process of differentiation of embryonic stem cells to neural stem cells (NSC). The transcriptome data were from Zhao et al (2015). R-NSCs are Rosette neural stem cells. Editing level of each cell was calculated as the average editing level of all RNA editing sites in the cell line.

Table S1. Genome coverage and the numbers of unique DNA mutations detected in each monkey tissue generated in this study.

Tissues	depth (x)	Unique mutations
heart	8.95	24977
liver	9.44	18188
spleen	10.06	26751
lung	9.7	23263
kidney	11.01	27998
testis	10.74	42317
prefrontal cortex	9.06	14861
hippocampus	8.93	23525
cerebellum	9.76	18733

Table S2. Summary of transcriptome data generated in this study used to call RNA editing

Tissue	Read Length	Read Number	Deduped Read Number
liver	100	96,492,296	45,927,481
muscle	100	63,241,952	28,615,300
heart	100	70,214,752	32,617,113
lung	100	29,412,420	19,841,034
spleen	100	68,544,376	40,913,854
kidney	100	73,889,386	52,208,722
testis	100	70,658,746	52,246,476
epididymis	100	54,708,652	36,360,540
retina	100	54,424,504	41,502,182
cerebrum	100	53,418,076	42,247,315
mesencephalon	100	68,796,616	48,317,495
cerebellum	100	84,378,358	65,161,284
thalamus	100	84,761,182	60,251,841
hypothalamus	100	76,449,952	51,477,149
occipital lobe	100	91,301,082	71,778,226
temporal lobe	100	69,768,640	53,476,032
frontal lobe	100	49,258,196	39,822,617
parietal lobe	100	64,642,084	50,447,621
inferior colliculus	100	48,123,288	38,547,272
superior colliculus	100	75,903,074	49,642,442
medulla oblongata	100	74,728,262	53,951,842
substantia nigra	100	51,994,364	36,031,194
olfactory bulb	100	63,475,838	49,668,227
globus pallidus	100	49,292,626	37,829,050
caudate nucleus	100	48,910,478	37,562,215
putamen	100	81,190,546	58,795,541
conarium	100	86,561,262	65,881,131
callosum	100	36,255,600	24,485,036
hippocampus	100	66,135,974	52,205,562
hypophysis	100	55,456,982	41,983,951

Table S3. Gene enrichment analysis of genes harboring editing sites with editing level that was positively correlated with *ADAR* expression.

Gene	*P*-value	Gene No.	term ID	GO term	Description
ADAR 1	2.73E-02	46	GO:0009894	BP	regulation of catabolic process
	1.83E-04	480	GO:0008152	BP	metabolic process
	1.06E-02	414	GO:0044237	BP	cellular metabolic process
	2.52E-02	93	GO:0044248	BP	cellular catabolic process
	5.32E-03	245	GO:0044710	BP	single-organism metabolic process
	2.30E-02	53	GO:0006396	BP	RNA processing
	1.06E-05	187	GO:0006996	BP	organelle organization
	1.56E-02	21	GO:0006399	BP	tRNA metabolic process
	2.44E-05	610	GO:0005623	CC	cell
	2.34E-05	609	GO:0044464	CC	cell part
	2.59E-02	70	GO:0097458	CC	neuron part
	3.64E-13	573	GO:0005622	CC	intracellular
	4.88E-15	567	GO:0044424	CC	intracellular part
	2.00E-11	462	GO:0005737	CC	cytoplasm
	4.13E-06	350	GO:0044444	CC	cytoplasmic part
	2.92E-04	164	GO:0005829	CC	cytosol
	8.08E-06	210	GO:0031974	CC	membrane-enclosed lumen
	3.33E-09	526	GO:0043226	CC	organelle
	1.01E-07	492	GO:0043227	CC	membrane-bounded organelle
	4.72E-10	496	GO:0043229	CC	intracellular organelle
	7.17E-09	459	GO:0043231	CC	intracellular membrane-bounded organelle
	2.72E-04	301	GO:0005634	CC	nucleus
	2.86E-03	95	GO:0005739	CC	mitochondrion
	1.23E-09	370	GO:0044422	CC	organelle part
	2.06E-05	206	GO:0043233	CC	organelle lumen
	2.56E-09	361	GO:0044446	CC	intracellular organelle part
	1.17E-05	205	GO:0070013	CC	intracellular organelle lumen
	4.47E-06	193	GO:0044428	CC	nuclear part
	8.20E-06	178	GO:0031981	CC	nuclear lumen
	1.31E-06	155	GO:0005654	CC	nucleoplasm
	8.39E-03	220	GO:0032991	CC	macromolecular complex
	1.59E-02	192	GO:0043234	CC	protein complex
	3.02E-04	550	GO:0005488	MF	binding
	1.15E-07	452	GO:0005515	MF	protein binding
	4.25E-02	70	GO:0042802	MF	identical protein binding
	1.73E-02	133	GO:0036094	MF	small molecule binding

	2.86E-02	120	GO:1901265	MF	nucleoside phosphate binding
	2.80E-02	120	GO:0000166	MF	nucleotide binding
	6.20E-03	90	GO:0003723	MF	RNA binding
	9.16E-07	265	GO:0003824	MF	catalytic activity
ADAR 2	2.57E-02	58	GO:0006396	BP	RNA processing
	2.00E-04	539	GO:0008152	BP	metabolic process
	2.65E-02	466	GO:0044238	BP	primary metabolic process
	1.23E-02	481	GO:0071704	BP	organic substance metabolic process
	2.87E-02	269	GO:0044710	BP	single-organism metabolic process
	1.51E-04	476	GO:0044237	BP	cellular metabolic process
	4.73E-03	106	GO:0044248	BP	cellular catabolic process
	6.18E-04	199	GO:0006996	BP	organelle organization
	1.40E-03	250	GO:0032991	CC	macromolecular complex
	4.89E-03	217	GO:0043234	CC	protein complex
	9.24E-04	682	GO:0005623	CC	cell
	1.43E-03	680	GO:0044464	CC	cell part
	2.13E-16	652	GO:0005622	CC	intracellular
	4.40E-18	644	GO:0044424	CC	intracellular part
	1.55E-11	517	GO:0005737	CC	cytoplasm
	2.55E-07	397	GO:0044444	CC	cytoplasmic part
	7.56E-10	250	GO:0031974	CC	membrane-enclosed lumen
	1.63E-13	605	GO:0043226	CC	organelle
	2.89E-02	191	GO:0043228	CC	non-membrane-bounded organelle
	1.26E-11	567	GO:0043227	CC	membrane-bounded organelle
	1.24E-16	578	GO:0043229	CC	intracellular organelle
	2.89E-02	191	GO:0043232	CC	intracellular non-membrane-bounded organelle
	3.35E-14	534	GO:0043231	CC	intracellular membrane-bounded organelle
	1.13E-08	358	GO:0005634	CC	nucleus
	3.71E-05	112	GO:0005739	CC	mitochondrion
	5.48E-17	440	GO:0044422	CC	organelle part
	5.43E-10	248	GO:0043233	CC	organelle lumen
	1.32E-16	430	GO:0044446	CC	intracellular organelle part
	2.27E-10	247	GO:0070013	CC	intracellular organelle lumen
	6.57E-11	233	GO:0044428	CC	nuclear part
	4.24E-10	214	GO:0031981	CC	nuclear lumen
	1.07E-11	189	GO:0005654	CC	nucleoplasm

	7.99E-04	172	GO:0031090	CC	organelle membrane
	3.70E-02	12	GO:0000792	CC	heterochromatin
	3.64E-05	287	GO:0003824	MF	catalytic activity
	1.16E-04	621	GO:0005488	MF	binding
	1.42E-04	491	GO:0005515	MF	protein binding
ADAR 3	1.93E-05	484	GO:0008152	BP	metabolic process
	2.94E-03	420	GO:0044238	BP	primary metabolic process
	1.42E-03	433	GO:0071704	BP	organic substance metabolic process
	3.00E-02	291	GO:0006807	BP	nitrogen compound metabolic process
	4.45E-03	119	GO:1901564	BP	organonitrogen compound metabolic process
	1.69E-02	81	GO:1901566	BP	organonitrogen compound biosynthetic process
	9.76E-04	50	GO:0009894	BP	regulation of catabolic process
	5.72E-05	426	GO:0044237	BP	cellular metabolic process
	2.41E-03	97	GO:0044248	BP	cellular catabolic process
	5.91E-04	45	GO:0031329	BP	regulation of cellular catabolic process
	2.39E-03	176	GO:0006996	BP	organelle organization
	1.50E-02	33	GO:0010498	BP	proteasomal protein catabolic process
	3.60E-03	33	GO:0043161	BP	proteasome-mediated ubiquitin-dependent protein catabolic process
	1.17E-06	613	GO:0005623	CC	cell
	2.56E-06	611	GO:0044464	CC	cell part
	1.21E-02	67	GO:0031975	CC	envelope
	2.62E-19	587	GO:0005622	CC	intracellular
	7.40E-21	580	GO:0044424	CC	intracellular part
	9.36E-13	466	GO:0005737	CC	cytoplasm
	1.62E-07	356	GO:0044444	CC	cytoplasmic part
	4.63E-02	153	GO:0005829	CC	cytosol
	1.47E-07	217	GO:0031974	CC	membrane-enclosed lumen
	3.08E-15	544	GO:0043226	CC	organelle
	3.60E-03	176	GO:0043228	CC	non-membrane-bounded organelle
	5.45E-13	510	GO:0043227	CC	membrane-bounded organelle
	1.54E-17	397	GO:0044422	CC	organelle part
	1.24E-06	211	GO:0043233	CC	organelle lumen
	1.44E-16	516	GO:0043229	CC	intracellular organelle

3.60E-03	176	GO:0043232	CC	intracellular non-membrane-bounded organelle
4.35E-03	105	GO:0005856	CC	cytoskeleton
2.30E-03	67	GO:0015630	CC	microtubule cytoskeleton
4.34E-18	391	GO:0044446	CC	intracellular organelle part
6.69E-07	210	GO:0070013	CC	intracellular organelle lumen
1.07E-02	67	GO:0031967	CC	organelle envelope
8.23E-14	476	GO:0043231	CC	intracellular membrane-bounded organelle
1.03E-07	317	GO:0005634	CC	nucleus
2.00E-08	202	GO:0044428	CC	nuclear part
2.19E-07	184	GO:0031981	CC	nuclear lumen
6.11E-09	163	GO:0005654	CC	nucleoplasm
4.58E-02	90	GO:0005739	CC	mitochondrion
1.71E-05	162	GO:0031090	CC	organelle membrane
2.46E-02	217	GO:0032991	CC	macromolecular complex
6.59E-05	256	GO:0003824	MF	catalytic activity
5.05E-03	113	GO:0016740	MF	transferase activity
3.77E-03	61	GO:0016772	MF	transferase activity, transferring phosphorus-containing groups
8.50E-03	49	GO:0016773	MF	phosphotransferase activity, alcohol group as acceptor
4.88E-03	54	GO:0016301	MF	kinase activity
3.13E-02	42	GO:0004672	MF	protein kinase activity
8.40E-03	35	GO:0004674	MF	protein serine/threonine kinase activity
3.85E-02	20	GO:0000287	MF	magnesium ion binding
3.19E-03	91	GO:0003723	MF	RNA binding
1.65E-02	70	GO:0044822	MF	poly(A) RNA binding
3.59E-06	557	GO:0005488	MF	binding
1.69E-03	264	GO:1901363	MF	heterocyclic compound binding
8.18E-08	452	GO:0005515	MF	protein binding
2.92E-02	91	GO:0019899	MF	enzyme binding
4.25E-03	269	GO:0043167	MF	ion binding
6.34E-03	135	GO:0043168	MF	anion binding
3.77E-03	265	GO:0097159	MF	organic cyclic compound binding
1.22E-03	126	GO:1901265	MF	nucleoside phosphate binding
5.51E-03	101	GO:0035639	MF	purine ribonucleoside triphosphate binding
6.09E-03	135	GO:0036094	MF	small molecule binding
8.85E-03	101	GO:0001882	MF	nucleoside binding
7.51E-03	101	GO:0032549	MF	ribonucleoside binding
7.51E-03	101	GO:0001883	MF	purine nucleoside binding

6.99E-03	101	GO:0032550	MF	purine ribonucleoside binding
1.19E-03	126	GO:0000166	MF	nucleotide binding
6.06E-03	103	GO:0017076	MF	purine nucleotide binding
1.23E-02	102	GO:0032553	MF	ribonucleotide binding
1.47E-02	101	GO:0032555	MF	purine ribonucleotide binding
3.11E-02	83	GO:0005524	MF	ATP binding

Gene Ontology (GO) term: BP- biological process; CC- cellular component; MF - molecular function.

Table S4. Gene enrichment analysis of genes containing editing sites with editing level that was positively correlated with age.

P-value	term ID	Type	Description	Genes
1.15E-02	GO:0035235	BP	ionotropic glutamate receptor signaling pathway	*ATP1A3*, *GRIA2*, *GRIA3*, *GRIK1*
8.01E-03	KEGG:04724	ke	Glutamatergic synapse	*PLA2G4C*, *GNB4*, *GRIA2*, *GRIA3*, *GRIK1*

Table S5. 75 RNA editing sites exhibit differential editing level between autism and control.

CHROM	POSITION	REF	ALT	REGION	GENE	STRAND
1	1316199	T	C	intronic	CPSF3L	-
1	1318414	T	C	intronic	CPSF3L	-
1	16563071	T	C	UTR3	NBPF1	-
1	19217289	T	C	UTR3	EMC1	-
1	32682570	A	G	UTR3	RBBP4	+
1	35602159	T	C	UTR3	PSMB2	-
1	35602220	T	C	UTR3	PSMB2	-
1	156406833	T	C	intronic	C1orf61	-
1	160095829	T	C	intronic	IGSF8	-
1	179073482	A	G	UTR3	FAM20B	+
10	6229872	A	G	intronic	PFKFB3	+
10	15077786	T	C	UTR3	ACBD7	-
10	73249834	T	C	ncRNA_UTR3	MRPS16	-
11	16756396	A	G	UTR3	C11orf58	+
11	78069071	T	C	UTR3	NDUFC2	-
12	12329641	T	C	UTR3	MANSC1	-
12	12329880	T	C	UTR3	MANSC1	-
12	50931505	A	G	UTR3	METTL7A	+
12	50931636	A	G	UTR3	METTL7A	+
12	120461371	A	G	UTR3	GATC	+
12	131848235	A	G	intronic	MMP17	+
13	49913203	T	C	UTR3	SPRYD7	-
14	26448324	T	C	exonic	NOVA1	-
14	73885182	A	G	UTR3	PTGR2	+
14	74059451	T	C	UTR3	ALDH6A1	-
14	74060281	T	C	UTR3	ALDH6A1	-
14	103684063	A	G	intronic	KLC1	+
15	41298646	A	G	ncRNA_exonic	OIP5-AS1	+
15	75353435	A	G	intronic	NEIL1	+
19	4653594	A	G	UTR3	TNFAIP8L1	+
19	4654525	A	G	UTR3	TNFAIP8L1	+
19	16550468	T	C	UTR3	SLC35E1	-
19	58263376	A	G	UTR3	ZNF544	+
2	37204331	A	G	ncRNA_exonic	CEBPZOS	+
2	37204342	A	G	ncRNA_exonic	CEBPZOS	+
2	37204458	A	G	ncRNA_exonic	CEBPZOS	+
2	37204461	A	G	ncRNA_exonic	CEBPZOS	+
20	3872213	A	G	UTR3	MAVS	+
3	10152310	A	G	UTR3	VHL	+
3	10153057	A	G	UTR3	VHL	+
3	10153300	A	G	UTR3	VHL	+
3	10153349	A	G	UTR3	VHL	+

	3	14944604	T	C	ncRNA_exonic	FGD5-AS1	-
	3	15072799	T	C	UTR3	RBSN	-
	3	15072810	T	C	UTR3	RBSN	-
	4	440777	T	C	ncRNA_UTR3	ZNF721	-
	4	17801353	T	C	UTR3	DCAF16	-
	4	56460122	A	G	UTR3	PAICS	+
	4	88259128	T	C	UTR3	PPM1K	-
	4	99880742	T	C	UTR3	LAMTOR3	-
	5	126626365	A	G	UTR3	PHAX	+
	5	126626861	A	G	UTR3	PHAX	+
	5	131953518	T	C	UTR3	ACSL6	-
	22	18924352	T	C	intronic	PRODH	-
	22	29439620	T	C	ncRNA_exonic	RFPL1S	-
	22	50442027	A	G	intronic	PPP6R2	+
	7	4769693	A	G	UTR3	FOXK1	+
	7	25121351	T	C	UTR3	CYCS	-
	7	25121461	T	C	UTR3	CYCS	-
	7	44041583	A	G	ncRNA_intronic	LINC00957	+
	7	44831055	T	C	intronic	H2AFV	-
	7	44833578	T	C	intronic	H2AFV	-
	8	38972958	A	G	UTR3	PLEKHA2	+
	8	43029280	A	G	UTR3	HOOK3	+
	9	128331576	A	G	intronic	COQ4	+
X		123912440	A	G	UTR3	XIAP	+
X		123913313	A	G	UTR3	XIAP	+
	1	145922089	T	C	ncRNA_UTR3	RBM8A	-
	15	90082890	T	C	downstream	ZNF710	+
	17	43766512	C	T	UTR3	DUSP3	-
	17	75064780	G	A	UTR3	KCTD2	+
	6	70588986	A	G	downstream	SDHAF4	+
	7	44062890	C	G	exonic	PGAM2	-
	7	44062905	C	T	exonic	PGAM2	-
	7	78017416	C	T	UTR3	MAGI2	-

CHROM: chromosome. REF are reference base, and ALT are alternative base.

Supplementary Table S6. Gene ontology analysis of genes harboring RNA editing sites exhibiting differential editing level between autism and control by DAVID program.

Category	Term	Count	*P*-Value	Genes	Benjamini correct *P*-value
UP_KEYWORDS	Mitochondrion	12	9.01E-05	*MAVS, COQ4, ALDH6A1, MRPS16, SDHAF4, PPM1K, CYCS, NDUFC2, ACSL6, PRODH, CEBPZOS, GATC*	0.011823
UP_KEYWORDS	Transit peptide	7	0.002237	*COQ4, ALDH6A1, MRPS16, SDHAF4, PPM1K, PRODH, GATC*	0.137408
GOTERM_CC_DIRECT	GO:0005739~mitochondrion	9	0.024493	*MAVS, COQ4, ALDH6A1, MRPS16, VHL, PPM1K, CYCS, PRODH, GATC*	0.8785
GOTERM_CC_DIRECT	GO:0005743~mitochondrial inner membrane	5	0.030462	*COQ4, MRPS16, CYCS, NDUFC2, PRODH*	0.731464
UP_SEQ_FEATURE	transit peptide:Mitochondrion	5	0.033861	*COQ4, ALDH6A1, MRPS16, PPM1K, PRODH*	0.999791
GOTERM_CC_DIRECT	GO:0005759~mitochondrial matrix	4	0.0576	*ALDH6A1, SDHAF4, PPM1K, PRODH*	0.81379
UP_KEYWORDS	Disease mutation	6	0.788525	*COQ4, ALDH6A1, VHL, CYCS, PGAM2, PRODH*	0.999341